Fritz Laboratory Reports

Civil and Environmental Engineering

1950

Shell arch roof model under simulated end wind load, June 1950

B. Thurlimann

B. G. Johnston

Follow this and additional works at: http://preserve.lehigh.edu/engr-civil-environmental-fritz-lab-reports

PROGRESS REPORT 213C

SHELL ARCH ROOF MODEL UNDER

SIMULATED END WIND LOAD

by

Bruno Thürlimann
Bruce G. Johnston

to

Roberts and Schaefer Engineering Company

Fritz Engineering Laboratory
Civil Engineering Department
Lehigh University
Bethlehem, Penna.

June 22, 1950

TABLE OF CONTENTS

Shell Arch Roof Model Under Simulated End Wind Load

by

Bruno Thürlimann and Bruce G. Johnston

Summary

Test results of a model of a shell roof, reinforced by ribs
in radial planes, (Fig. 1) under 3 different cases of end loads
(Fig. 2) are presented. A theoretical study of one of the cases
(uniform end load) is made. To overcome the mathematical
difficulties, simplifications are introduced. A fairly good
agreement between test results and analysis is established.

Introduction

Horizontal end loads on shell arch roof buildings, due
primarily to wind forces, represent loading conditions which
have had little attention in the literature. Aas - Jakobsen (1)*
analyses the horizontal wind pressure on arch-bridges. His method
suggests some ideas which may be of use in the present problem,
but it has to be extended to take into consideration the inter-
action between ribs and shell. The latter is done in a fairly
simple way, taking the "effective width" (2)* of the shell as
a flange of the ribs. The forces in the shell are found by
procedures similar to those used in the previous two reports
(2,3)*

- -

* (1), (2) See list of references at end of report.

Part I: Theoretical Analysis

1.   Problem Simplification:

A uniform horizontal load is assumed as acting on the shell (Fig. 2a).   A part of length $R_S d\omega$ is cut out and the two outer ribs are arbitrarily separated from the shell (Fig. 3b).   Assuming that in this state the shell carries shear forces only, (and that $\frac{\partial T_1}{\partial x}$ is constant), then from Fig. 3a:

$$\frac{dS}{dx} = 0$$

$$S = f(\omega) \tag{1}$$

No distinction between the shear forces S_{12} and S_{21} in the $R_S\omega$ and x- directions has been made: $S_{12} = S_{21} = S$.   The significance of this simplification is discussed in Ref. (4), p. 117.   By Eq. (1) (assuming $\frac{\partial T_1}{\partial x}$ a constant), S is a function of ω only, therefore it is constant along a cut $\omega =$ constant over the depth h of the shell.   The equilibrium of the free body diagram Fig. 3b requires:

$$\frac{dS}{d\omega} = -\frac{R_S}{h} p$$

$$S = -\frac{R_S}{h} p\omega \tag{2}$$

The constant of integration is zero since for $\omega = 0$ symmetry requires $S = 0$.   To keep the shell element of Fig. 3b in equilibrium, shear forces must act along $x = 0$ and $x = h$. These act as reactions along the outer ribs as shown in Fig. 3b.

To eliminate the relative displacements between ribs and shell, introduced by cutting these two elements arbitrarily

apart, redundant forces Y (see (3), p. 4) are introduced.
The condition of equality between the strains of the shell
and the ribs determines the magnitude of Y.

For practical purposes the above procedure is too
elaborate (see example in Progress Report 213-B). The
interaction between rib and shell can be taken care of by
introducing the effective width of the shell as a flange
of the rib. The stresses and deflection of the rib under
the action of the shear forces S are in the following two
cases the same:

Case 1: Rib and shell cut apart. Action of S on the rib
only. Elimination of the relative displacement
between rib and shell by the redundant force Y.
(Fig. 5a).

Case 2: Action of S on the rib of a cross-section consisting
of the rib and a flange of width equal to the effect-
ive width of the shell. (Fig. 5b).

The analysis of "Case 2" can be done by ordinary arch theory.
The effective width b is determined from the diagram in
Ref. (3), Fig. 8. The only difficulty consists in predicting
in advance the coefficient λ (depending on the force distri-
bution), and the numerical example in Part II shows that
this easily is accomplished.

The forces in the shell due to the interaction of
rib and shell, are found by the following simple procedure.
In Ref. (3), eq. (36), p. 23, the effective width is of the
form:

$$b = \frac{Y}{T_2} \text{ (at rib)}$$

Knowing the stresses in the rib, T_2 at $x = 0$ can be calculated:

$$T_2 = \sigma_s d$$

> where: d = thickness of the shell
>
> σ_s = normal stress in rib in the fiber of the connecting line rib-shell

The "string force Y" reduces to:

$$Y = bd\sigma_s \tag{3}$$

It remains to study the shell under the action of the string force Y, a problem already solved in Progress Report 213-B. The example in Part II illustrates the practical solution.

If the interior rib is placed exactly in the middle between the two outer ribs, it is of no influence on the stress distribution in the structure. Consideration of symmetry shows (Fig. 3b) that the displacements v and w of the middle rib are zero. If the torsional stiffness and the bending stiffness in x-direction (small I) are disregarded, no stresses will be produced in it. Therefore, the middle rib may be considered as not present in the analysis of horizontal loads acting on the shell. (See test results as further justification of this statement.)

A further point of discussion is the question of the T_1 forces (direct forces in x-direction) due to the loads p (Fig. 3b). Two extreme cases may be distinguished:

1. p acting as compression at $x = 0$ (as shown in Fig. 3b).

2. p acting as tension at $x = h$.

If the depth "h" of the shell is small compared to the span
of the arch roof, the problem may be answered by the same
reasoning as in beam theory. Fig. 4 shows how the two cases
can be built up by simple superposition. The straight line
distribution is a close approximation under the above given
assumption (small depth h). With the same justification
as in the case of the normal stresses in the vertical
direction in the web of an I-beam, the deformations caused
by the T_1 forces are neglected. Their maximum value (at
x = 0 or x = h) is easily determined from the boundary
conditions.

2. Edge-Member Disturbance and the Restraint of the Ribs
by the Abutments:

The conditions at the springing line require some
special attention. The rib rises from a heavy end wall
(Fig. 1). It may be considered as fully restrained by this
wall. On the other hand, the shell rests on a flexible
edge-member. It is proposed to take care of these influences
by an approximate solution.

Two limiting cases are considered:

1. Rigid edge-member ⎫
                        ⎬ rib fully restrained
2. No edge-member   ⎭

In the first case, the section consisting of the rib and
a flange of width b (effective section)* is fully restrained
as a whole (Fig. 6b). In the second case the effective

- -

* By "effective section" of the rib, the cross section consisting
  of the rib and a flange of width equal to the effective width
  is meant. On the following pages the term is used with this
  meaning.

width b has to reduce to zero at the springing line
(Fig. 6c). The determination of this reduction is a
problem in itself. It may be by-passed by the assumption
that the full effective width acts down to the edge-
member, but   the section of rib and flange b as a
whole (effective section) is elastically restrained at the
abutment. The reduction of the moment of inertia of the
effective section in the end zone is concentrated arbitrarily
at the springing line. By St. Venant's principle, this
simplification results only in local differences of the
actual state of stress.

In a general case, when the shell is supported by
a flexible edge-member, the effective width b does not
reduce to zero completely, and the elastic restraint of the
effective section is higher than in Case 2.

The determination of the coefficient of elastic
restraint κ offers certain difficulties. Further theoreti-
cal studies of the edge-member problem may lead to an
explicit expression for κ . For the present Hangar model
(Fig. 1) $\kappa = 0.2 \dfrac{R_\theta}{EI}$. If a moment $M_k = -1$ is applied
to the support, the latter rotates through an angle of κ
radians (Fig. 7). The angle of rotation of the support
due to an end moment is

$$\phi_k = -\kappa M_k \qquad (4)$$

The two limiting cases for κ are:

$\kappa = 0$: Fully restrained arch

$\kappa = \infty$: Two-hinged arch

For the practical application of this procedure, reference is made to the numerical example in Part II.

If the numerical procedure of integration in the arch analysis is used (as in most actual problems), the reduction of the moment of inertia of the effective section in the edge-member zone can be considered directly. Still, certain assumptions about the reduction of the effective width b have to be made (curve of b in Fig. 6c).

3. <u>Calculation of the Rib Stresses</u>:

The shear forces S offer a rather unfamiliar type of loading in the arch theory. Statically speaking, the rib forms an elastically restrained arch. A cantilever is chosen as the statically determinate base system (Fig. 8a). The number of the redundant forces reduces to two, horizontal thrust H_c and M_c at the center.

The normal force N_0 and the bending moment M_0 in the statically determinate base system (Fig. 8a and 8b) may be obtained by integrating the contribution of the distributed shear load that is applied by the shell to the effective rib section. If ω is the angle at which N_0 and M_0 are determined, let $SR_S d\alpha$ represent the shear load applied over incremental shell distance at any angle α between 0 and ω. (Fig. 8b). Then,

$$N_0 = - \int_0^\omega SR_S \cos(\omega - \alpha)d\alpha$$

Substituting from Eq. 2, $S = - \dfrac{R_S p \alpha}{h}$ and performing the integration,

$$N_0 = \frac{R_S^2 p}{h}(1 - \cos\omega) \qquad (5)$$

Similarly, the contribution to the moment M_0 of incremental

shear load is $SR_S d\alpha$ multiplied by the moment arm

$y_s = R_e \left[1 - \cos(\omega - \alpha) \right]$ as shown in Fig. 8b. The integrated

total of M_0, then is,

$$M_0 = - \int_0^\omega SR_S \left[y_s - R_e \left(1 - \cos(\omega - \alpha) \right) \right] d\alpha$$

substituting as before for S and integrating,

$$M_0 = \frac{R_S^2 R_e P}{h} \left[\left(\frac{y_s}{R_e} - 1 \right) \frac{\omega^2}{2} + 1 - \cos\omega \right] \qquad (6)$$

The normal force N and the bending moment M in the arch

are:

$$N = N_0 - H_c \cos\omega \qquad (7)$$

$$M = M_0 + H_c R_e (1 - \cos\omega) + M_c \qquad (8)$$

The boundary conditions for $\omega = \omega_k$ determine the redundants

H_c and M_c:

$$\omega = \omega_k: \qquad \delta_k = 0$$

$$\phi_k = - \kappa M_k$$

Where: δ_k = horizontal displacement of

the support

ϕ_k = rotation of the support (Fig 7)

M_k = moment M for $\omega = \omega_k$

Fig. 8c and 8d show the virtual load system used to find

the above deformations:

For δ_k (Fig. 8c): $M' = - R_e (\cos\omega - \cos\omega_k)$ (9)

For ϕ_k (Fig. 8d): $M' = 1$ (10)

For the determination of H_c and M_c the deformations caused by

the normal forces are disregarded.

Applying the work equation

$$\delta = \int \frac{M'Mds}{EI}$$

δ_k and ϕ_k follow to:

Eq. 8 & 9: $\quad \delta_k = \int\limits_0^{\omega_k} \frac{1}{EI} \left[- R_\theta(\cos\omega - \cos\omega_k) \right] \cdot \left[M_0 \mp H_c R_\theta(1-\cos\omega) \right.$

$$\left. + M_c \right] R_\theta d\omega$$

Eq. 8 & 10: $\quad \phi_k = \int\limits_0^{\omega_k} \frac{1}{EI} \left[M_0' \mp H_c R_\theta(1-\cos\omega) + M_c \right] R_\theta d\omega$

If EI is constant, the integration can be performed:

$$-\delta_k \frac{EI}{R_\theta^2} = M_c(\sin\omega_k - \omega_k \cos\omega_k) + H_c R_\theta(\sin\omega_k + \frac{1}{4}\sin 2\omega_k$$

$$-\frac{1}{2}\omega_k - \omega_k\cos\omega_k)$$

$$-\frac{R_S^2}{h}p\, R_\theta \left[(1 - \frac{y_s}{R_\theta})(\omega_k\cos\omega_k + (\frac{\omega_k^2}{2} - 1)\sin\omega_k - \frac{\omega_k^3}{6}\cos\omega_k) \right.$$

$$\left. - \sin\omega_k - \frac{1}{4}\sin 2\omega_k + \frac{1}{2}\omega_k + \omega_k\cos\omega_k \right] \tag{11}$$

$$\phi_k \frac{EI}{R_\theta} = M_c\omega_k + H_c R_\theta(\omega_k-\sin\omega_k) - \frac{R_S^2}{h}p\, R_\theta \left[(1-\frac{y_s}{R})\frac{\omega_k^3}{6} - \omega_k + \sin\omega_k \right] \tag{12}$$

Eq. (11) and (12) are 2 linear equations with 2 unknowns
M_c and H_c, the solution of which is dealt with in the numerical
example, Part II.

The values of δ_k and ϕ_k depend on the support conditions
of the ribs:

1. Fully restrained arch:

$$\omega = \omega_k: \qquad \delta_k = 0$$

$$\phi_k = 0$$

2. Elastically restrained arch: (See Eq. (4))

$$\omega = \omega_k: \qquad \delta_k = 0$$

$$\phi_k = - \kappa M_k$$

Knowing H_c and M_c, the actual normal force N and the actual moment M are determined by eq. (7) and (8). Concerning the cross section of the rib, it was shown under I, 1., that the combined action of rib and shell can be taken into account by using the "effective cross section".*

4. Deflection of the Ribs:

The calculation of the deflections of the ribs is obtained by numerical use of the work equation.

A few words may be said about the two load-systems determining the M, N and the M', N' respectively.

Actual load-system: The M and N are the moment and normal force as determined by eq. (7) and (8) for the actual structure under the actual load.

Virtual load system: The M' and N' are the moment and normal force due to a virtual load P = 1 at the point of the deflection under investigation and in its direction. The virtual structure has to be identical to the actual one except for the boundary conditions. Usually they are chosen so as to make the work of the support forces equal to zero. Fig. 9 illustrates the two systems for the present case.

Part II: Numerical Analysis

The successive steps in analyzing a shell-roof of the present type (Fig. 1) consist in the determination of:

1. Shear forces S , eq. (2)

2. Effective width b , effective cross-section*

3. Analysis of the effective cross section as an arch under loads S

---

* See footnote on page 5.

4. Deflection of arch rib

5. String force Y, eq. (3)

6. Shell forces due to the string force Y

List of the principal dimensions and datas (Fig. 1):

Outer ribs: Radius $R_R = 109.06"$

Height $h_R = 2.113"$

Thickness $b_R = 0.505"$

Angle $\omega_k = 0.5866^{\pi} radians$

Shell: Radius $R_S = 108"$

Thickness $d = 0.118"$

Depth of Shell $h = 24"$

Load*: $p = 140.62$ lb/in

Measured support movements: $\delta_k = -1.03 \cdot 10^{-2}$ in

$\phi_k = 1.074 \cdot 10^{-3}$ radians

1. Shear forces S:

Eq. (2): $S = -\dfrac{R_S}{h} p \omega = -\dfrac{108}{24} \omega \cdot 140.62 = -\underline{632.79\, \omega}$

2. Effective width b, effective cross section:

Effective width b:

Fig. 8, Progress Report 213-B gives the effective width b as function of the two parameters λ and (βx). The present structure has no overhang, hence $(\beta x) = 0$. The distance "h" between the two outer ribs is wide enough, so that there is no appreciable interaction between them, and the shell may be considered as infinitely long. For $(\beta x) = 0$, a variation of the parameter λ from 0 to 0.5 results in a

---

* In the test, the load was actually tension along the rib x = h. But as seen under I, 1., compression loads at x = 0 and tension loads at x = h produce essentially the same state of stress except for the T_1 -forces (see Fig. 5).

variation of the coefficient K from 0.3799 to 0.3665, or

3.5%. The determination of the coefficient c requires the

knowledge of the force distribution along the connecting

line rib-shell. For a shell roof of the present type under

uniform lateral wind load, an approximation is:

$$c \cong \frac{3\pi}{2\omega_k} = \frac{3\pi}{2 \cdot 0.5866} = 8.0334^*$$

Coefficient λ : $\lambda = c \sqrt{\frac{d}{R}} = 8.0334 \sqrt{\frac{0.118}{108}} = \underline{0.26554}$

λ is in any case smaller than 0.5. The K-value for

$\lambda = 0$ is therefore sufficiently accurate.

$$\left. \begin{array}{l} \lambda = 0 \\ \\ (\beta x) = 0 \end{array} \right\} \quad \begin{array}{l} K = 0.3799 \\ \\ b = K\sqrt{Rd} = 0.3799 \sqrt{108 \cdot 0.118} = \underline{1.3562} \end{array}$$

In summary, the procedure of finding "b" consists in a test

of λ. If $\lambda < 0.5$ (as is usually the case for shell-roofs

of the present type under uniform horizontal load p), the

K-value for $\lambda = 0$ gives a very close approximation for the

determination of the effective width.

Effective cross-section:
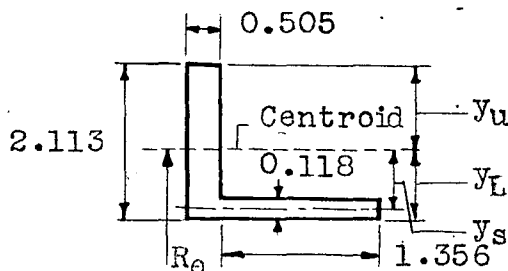
Area:
$$A = 2.113 \cdot 0.505 = 1.0671$$
$$+ 0.118 \cdot 1.356 = 0.1600$$
$$A = 1.2271 \text{ in}^2$$

---

* See Fig. 13, where the stress σ_L has the variation of a
cosine function of half-wave length of about $= 0.35 \div 0.40$:

$$c = \frac{\pi}{2} \cdot \frac{\lambda}{\text{half-wave length}} \cdot$$

Centroid: $Q = 0.1600 \cdot 0.5(2.113 - 0.118) = 0.1597$ in^3

$$x = \frac{Q}{A} = \frac{0.1597}{1.2271} = 0.1301 \text{ in}$$

$$y_u = 0.5 \cdot 2.113 + 0.1301 = \underline{1.1861 \text{ in}}$$

$$y_L = 0.5 \cdot 2.113 - 0.1301 = \underline{0.9259 \text{ in}}$$

$$y_s = 0.9259 - 0.5 \cdot 0.118 = \underline{0.8669 \text{ in}}.$$

Radius of effective rib-section: $R_e = R_s + y_L = 108 + 0.9259$

$$= \underline{108.926 \text{ in}}$$

Moment of Inertia: $I = \dfrac{b_R h_R^3}{12} = \dfrac{1}{12} \cdot 0.505 \cdot 2.113^3 = 0.3970$

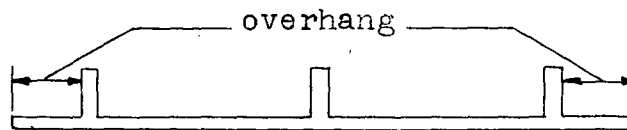$$+ a_1^2 A_1 = 0.1301^2 \cdot 1.0671 = 0.0181$$

$$+ a_2^2 A_2 = 0.8669^2 \cdot 0.1600 = \underline{0.1205}$$

$$I = \underline{0.5356 \text{ in}^4}$$

Ratio $\dfrac{I \text{ (effective cross section)}}{I \text{ (rib only)}} = \dfrac{0.5356}{0.3970} = \underline{1.35}$

NOTE

The shell increases the bending stiffness of the ribs by 35%. An overhang of the shell could improve the stiffness up to about 100%. The importance of an overhang becomes apparent here again.

overhang

---

3. **Analysis of the ribs (effective cross section):**

Solution of the Eq. (11) and (12) for M_c and H_c:

List:*

$\omega_k = 0.5866$	$\sin \omega_k = 0.5535\,326$
$\omega_k^2 = 0.3440\,996$	$\cos \omega_k = 0.8328\,275$
$\omega_k^3 = 0.2018\,491$	$\sin 2\omega_k = 0.9219\,944$

- -

* The different terms of (11) and (12) are small differences of large numbers, therefore 7 decimal places are taken.

$$R_\theta = 108.926 \text{ in} \qquad (1 - \frac{y_s}{R_\theta}) = 1 - \frac{0.8669}{108.926} = 0.9920\ 41$$

$$R_\theta^2 = 1.1864\ 87.10^4 \text{ in}^2 \qquad \frac{EI}{R_\theta} = \frac{30.10^6 \cdot 0.5356}{108.926} = 1.4751 \cdot 10^5$$

$$R_S = 108 \text{ in} \qquad \frac{EI}{R_\theta^2} \quad \frac{30.10^6 \cdot 0.5356}{1.186487.10^4} = 1.3543 \cdot 10^3$$

a) Fully restrained arch:

Boundary conditions: $\omega = \omega_k$: $\qquad \delta_k = 0$

$$\phi_k = 0$$

Replacing in (11) and (12) the values listed above with

the given boundary conditions, they reduce to:

(11) $0.064996\ M_c + 0.23905\ H_c = 50.214$

(12) $0.5866\ M_c + 3.6019\ H_c = 1996.0$

And the solution:

$$\underline{M_c = -3155.9 \text{ in-lb}}$$

$$\underline{H_c = +1068.1 \text{ lb}}$$

b) Elastically restrained arch:

Boundary conditions: $\omega = \omega_k$: $\qquad \delta_k = -1.03 \cdot 10^2 \text{ in}$

$$\phi_k = 1.074 \cdot 10^{-3} - \kappa M_k$$

where $-1.03 \cdot 10^{-2}$ in. and $1.074 \cdot 10^{-3}$ radians are the

actually measured displacement and rotation of the support

respectively. The term κM_k takes care of the edge-member

action as explained in I, 2., p. 5 . ($\kappa = 0.2 \frac{R_\theta}{EI}$)

Eq. (11) and (12) become:

(11) $0.064996 M_c + 0.23905 H_c - 50.214 = \frac{EI}{R_\theta^2} 1.03 \cdot 10^{-2}$

(12) $0.5866 M_c + 3.6019 H_c - 1996.0 = \frac{EI}{R_\theta} (1.074 \cdot 10^{-3} - 0.2 \frac{R_\theta}{EI} M_k)$

M_k is the bending moment at the support $\omega = \omega_k$

From Eq. (8):

$$M_k = - 24791.42 + 18.209 \, H_c + M_c$$

(11) $\quad 0.064996 \, M_c + 0.23905 \, H_c = 64.163$

(12) $\quad 0.7866 \, M_c + 7.2437 \, H_c = 7112.7$

$$\underline{M_c = - 4370.6 \text{ in-lb}}$$

$$\underline{H_c = + 1456.7 \text{ lb}}$$

Fiber stresses in the ribs:

Knowing the normal force N (from eq. (7) and the bending moment M (from eq. (8), the fiber stresses σ_u (upper edge) and σ_L (lower edge) are found using the formula:

$$\sigma_u = \frac{N}{A} - \frac{My_u}{I}$$

$$\sigma_L = \frac{N}{A} + \frac{My_L}{I}$$

Tables I to III show the calculations.

4. Deflection of the ribs:

The deflection of the rib at $\omega = 0$ is calculated. Fig. 9 shows the two load systems used in the work equation:

Virtual load system: $P = 1$

$$M' = \frac{R_e}{2} (\sin \omega_k - \sin \omega)$$

$$N' = - \frac{1}{2} \sin \omega$$

Actual load system:

Elastically restrained ribs. M and N as given in Table II.

Work Equation:

$$\delta = 2 \int_0^{\omega_k} \frac{M'M ds}{EI} + 2 \int_0^{\omega_k} \frac{N'N ds}{EA} \cong \frac{2\Delta s}{EI} \left(\Sigma M'M - \frac{I}{A} \Sigma N'N \right)$$

Table IV gives the numerical calculations. The interval Δs is constant from $\omega = 0$ to $\omega = 0.5796$; the last interval is shorter. The summation is done by using the Trapezoid-formula.

$$\Delta s = R_\theta \Delta \omega$$

Path ω	$\Delta\omega$	Δs	$\Sigma M'M$	$\Sigma N'N$	$2\Delta s \Sigma M'M$	$2\Delta s \Sigma N'N$
0 to 0.5796	0.058	6.318	-10.193	-61.191	-128.80	-773.21
0.5796 to 0.5866	0.007	0.762	- 0.052	-28.010	- 0.07	-39.89
					-128.87	-813.10
Multiplier			10^4	10^2	10^4	10^2

$$\frac{I}{A} = \frac{0.5356}{1.2271} = 0.4365$$

$$2\Delta s \Sigma M'M = \qquad\qquad = -128.87 \cdot 10^4$$

$$\frac{I}{A} 2\Delta s \Sigma N'N = -0.4365 \cdot 813.10 \cdot 10^2 = - 3.55 \cdot 10^4$$

Deflection δ at center, $\omega = 0$:

Taking $E = 30 \cdot 10^6$ lb-in^{-2}:

$$\delta = \frac{-132.42 \cdot 10^4}{30.10^6 \cdot 0.5356} = -8.241 \cdot 10^{-2} \text{ in.}$$

Taking $E = 29 \cdot 10^6$ lb-in^{-2}

$$= \frac{-132.42 \cdot 10^4}{29.10^6 \cdot 0.5356} = -8.525 \cdot 10^{-2} \text{ in}$$

Comparison to test results:

Measured: $\delta = -9.10 \cdot 10^{-2}$ in (Rib $x = 0$)

Difference to analytical result:

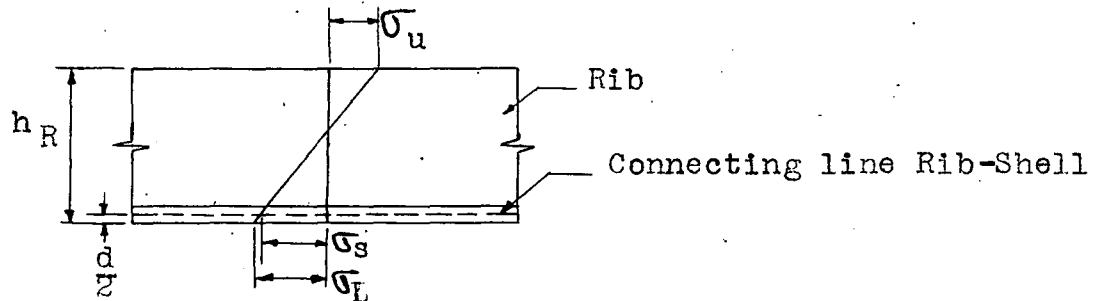For $E = 30.10^6$ lb-in^{-2}: $\Delta = -9.4\%$

For $E = 29.10^6$ lb-in^{-2}: $\Delta = -6.3\%$

5. <u>Determination of the string force Y:</u>

Eq. (3): $Y = bd\sigma_s$

b may be taken as constant over the entire span, with

exception of the end-zones. σ_s is the stress in the

connecting line rib-shell.

$$\sigma_s = \sigma_L - (\sigma_L - \sigma_u)\frac{d}{2h_R} = \sigma_L - (\sigma_L - \sigma_u)\frac{0.118}{2 \cdot 2.113}$$

$$\sigma_s = \sigma_L - 0.028(\sigma_L - \sigma_u)$$

The direct force T_2 in the shell (in circumferential direction)

at x = 0 is:

$$T_2\Big|_{x=0} = \sigma_s d$$

In Table V the $T_2\Big|_{x=0}$ and the Y are calculated for values

of ω between $\pm$ 0.4637. For the end-zone ω = 0.4637 to 0.5866,

the influence of the edge-member distrubance modifies the

stress distribution in the shell. No shell-forces are computed

for this part. Only the case of the elastically restrained

ribs is considered.

6. <u>Forces in the shell</u>

Knowing the string force Y applied to the shell at the

boundaries x = 0 and x = h (Fig. 3), the forces in the shell

can be calculated by the procedure developed in Progress Report

213-B. Comparing the normal forces T_2 and the bending moment

M_1 resulting from a unit string force Y = 1 (constant) or

$Y = 1 \cos(c\omega)$ respectively, applied at the edge of a semi-

infinite cylinder, it may be seen, that the difference in the results is very small, as long as c is not too large (See (3), Tables II, p. 54 and Tables IV, p. 57 respectively). Therefore the T_2 and M_1, due to a unit force Y, will be computed for Y = 1 (constant) only.

The thickness d and the radius R of the shell are the same as for the Pilot model, investigated in Progress Report 213-B, so that the values of Table IV of this report (3) can be used directly.
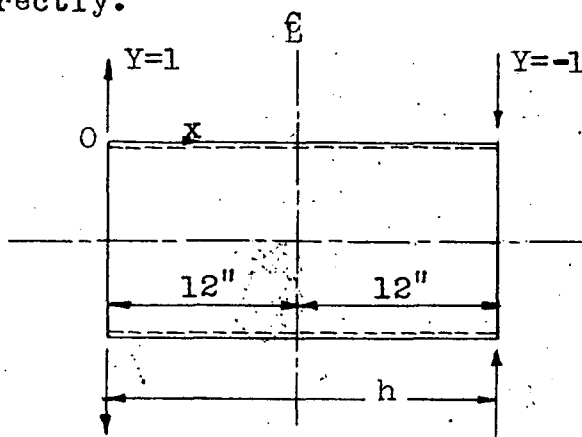
The sketch shows, how the shell is loaded by string forces Y = 1 at the edge x = 0 and Y = -1 at the edge x = h respectively (Fig. 3, for example, illustrates, that the loading of the outer ribs is anti-symmetric about the middle rib). To find the actual T_2 and M_1, the values due to the unit Y-Force are multiplied by the actual Y-Force. The calculations are made in Table VI.

Part III.   Experimental Investigation

1.   Description of Model and Test Set-up

The test structure represents a model in the approximate scale 1:30 of an actual shell-roof (e.g. hangar at Rapid City, South Dakota). Fig. 1 gives the actual dimensions. As a

material, steel was chosen in order to have nearly perfect
elasticity as is desirable for checking theoretical stress
analyses. Reinforced concrete would require a model of a
much larger size and would make an interpretation of the
electric strain gage readings almost impossible, due to
the combined effects of elasticity, plastic flow, shrinking,
and non-homogeneity of the material. The present model
exhibits nearly the properties assumed in the theoretical
analysis, i.e. linear elasticity.

The horizontal load p, assumed uniformly distributed
over the length of the rib, was applied by 10 concentrated
loads P (Fig. 2). The loads were produced by weights (water
buckets), applied to a lever-system with an advantage 1:7.5.
Wire cables passing over pulleys with roller bearings changed
the direction of the vertical load to a horizontal one,
as may be seen in Fig. (10).

The strains were measured by means of SR-4 electrical
strain gages. The lay-out of the gages is shown on Fig. 11.
A total of 44 rosette (type AR-1), 137 cross (AX-5) and 81
single (A-5) gages were applied. Two strain indicators
were used to take the 487 readings.

Dial gages measured the vertical displacements of the
outer ribs at 10 points and the lateral displacements of the
shell at 5 points (Fig. 12) (accuracy $\frac{1}{1000}$ in). The angular
displacements were recorded by level bars (accuracy $\frac{1}{20000}$
radian). Finally, the horizontal displacement of the
supports were measured by a dial gage.

2. <u>Test Procedure:</u>

Before the actual test, the model was subjected several times to a load of 1875 lb. per one loading point (10 loading points = 10 x 1875 lb.). With this procedure plastic flow, due to residual welding stresses, could be eliminated prior to the test.

The loads in the actual test were kept at 1687.5 lb. (90% of the first load) in order to keep away from every possible yielding. An initial set of readings was taken at zero load (shell under load of the loading system only). Then the loads (bucket + water = 225 lb.) were applied slowly up to the said load of 1687.5 lb. (lever advantage 1:7.5) for each loading point, and all readings were taken. This procedure was repeated once, to check all readings carefully. The applied load of 10 x 1687.5 lb. corresponds approximately to a uniformly distributed load of $p = \frac{1687.5}{12} =$ 140.62 lb. per one inch length of rib. This latter figure was used in the analysis.

3. <u>Test results</u>

All test results are recorded, including the two other load cases (2 concentrated loads in the middle, concentrated load at the quarter point), in the appendix to Progress Report 213-C "Test Results for 3 Cases of Lateral Loads on a Model of an Arch Roof".

In order to compare the analytical values with the test results, the stresses in the ribs, the moments M_1, and the direct forces T_2 in the shell were computed on the basis of the recorded strains. The disturbance due to edge-

member action was not studied in the analysis as far as the forces in the shell are concerned. Therefore no shell forces and moments in the edge-member region are worked out from the test results ($\omega = 0.4637$ to $\omega_k = 0.5866$).

4. Comparison between Test Results and Analysis:

The analysis was made under the following simplifying assumptions:

1. The edge member disturbance is taken into account by a coefficient of elastic restraint k for the ribs (See p. 5). No attempt is made to compute the shell-forces, due to edge-member action.

2. For the determination of the effective width, the shell moments M_2 and Piosson's ratio v were assumed to be zero (See (3), p. 6). The influence of the parameter λ (force distribution factor) was disregarded. (See p. 11).

3. The noraml forces T_2 and the M_1 in the shell were computed by an approximate method (See p. 17).

4. The torsional stiffness of all the ribs was disregarded.

Considering these simplifications, the comparison between test and analysis seems satisfactory. Fig. 13 shows the fiber stresses σ_u (upper) and σ_L (lower) in the ribs. The assumption of fully restrained ribs (ribs and shell are rigidly supported by the abutments) leads to stresses too low in the middle ($\omega = 0$) and too high at the support ($\omega = \omega_k$). The stresses computed for elastically restrained ribs (the edge-member provides only an elastic support of the shell) check very closely with the measured ones. As said before (p. 7), the actual determination of the coefficient of elastic restraint offers certain difficulties. It is believed, that

for the present type of a shell construction $K = 0.2 \frac{Re}{EI}$
is a very reasonable assumption. Despite this imperfection,
Fig. 13 demonstrates that the analytical attack, presented
in this report, gives the right functional correspondence
between structure and load. The analysis is based on
theoretical considerations except for the empirical evaluation
of the restraint coefficient " K ".

Normal force T_2 and bending moment M_1 of the shell
are presented in Fig. 14. In general, analytical and
experimental values check fairly well. A few experimental
points are quite far off. The following effects may offer
an explanation of these discrepancies: error in the strain
recording system, difference between actual and assumed
dimensions (e.g. shell actually has a curvature in x-direction,
which theoretically is taken as 0), concentrated loads P
instead of the assumed uniformly distributed load P (Fig. 2).
No attempt is made to give an explanation for each individual
point. It is possible that later tests will throw some
light on this question.

The deflection was checked analytically only at the
middle ($\omega = 0$). The correspondence is quite acceptable,
depending on the modulus of elasticity $E = 29$ to $30 \cdot 10^6 \, lb/in^2$
taken. The following table compares the results:

| | ANALYSIS | | TEST |
	$E = 29 \cdot 10^6$	$E = 30 \cdot 10^6$	
Rib x = 0	-0.0853 in	-0.0824 in	-0.0910 in
Rib x = h	0.0853 in	0.0824 in	0.0988 in

Vertical Deflection of Outer Ribs at $\omega = 0$ (middle)

Summarizing, the test furnished results corresponding fairly well with the analytical computations. The analysis, brought forward in this report, describes satisfactorily the actual state of stress in an arch-roof construction of the present type (span of the shell $\gg$ distance between the ribs).

5. <u>Relation Between the Model and an Actual Structure:</u>

To get the full advantage of the present experimental and theoretical study of the model in application to an actual structure, the knowledge of a few inter-relations between model and original may be very useful. No attempt is made to give a complete study of this relationship. The effective Poisson Ratio in the concrete structure is less than that of steel. The concrete of the original is supposed to have a perfect elastic behavior. This assumption is usually made as far as the calculation of the <u>direct forces</u> and <u>bending moments</u> in a reinforced concrete structure are concerned. (Shrinkage too, is considered as a load, due to a fictitious temperature change, on a <u>elastic</u> structure.) The assumption of the cracked tension-zone in the concrete is only made for the determination of the <u>reinforcement</u> and the <u>concrete stresses.</u>

A direct relation between a steel-model and a concrete original is possible under the above assumption of elastic behavior of the concrete. The following table gives the most important results.

	MODEL	ORIGINAL
Material	Steel	Concrete
Modulus of Elasticity	$E_{Mod} = 30 \cdot 10^6$ (lb/in²)	E_{Orig}
Given relations:		
Length	l_{Mod} (in.)	$l_{Orig} = n \cdot l_{Mod}$
Load per unit length	p_{Mod} (lb/in.)	$p_{Orig} = p_{Mod}$
Ribs:		
Normal Force N	N_{Mod} (lb.)	$N_{Orig} = n \cdot N_{Mod}$
Bending Moment M	M_{Mod} (in./lb.)	$M_{Orig} = n^2 \cdot N_{Mod}$
Shell:		
Normal Force T	T_{Mod} (lb/in.)	$T_{Orig} = T_{Mod}$
Bending Moment M	M_{Mod} (in./lb/in.)	$M_{Orig} = n \cdot M_{Mod}$
Stresses	σ_{Mod} (lb/in².)	$\sigma_{Orig} = \frac{1}{n} \cdot \sigma_{Mod}$
Deflections	δ_{Mod} (in.)	$\delta_{Orig} = \frac{E_{Mod}}{E_{Orig}} \delta_{Mod}$

The application of this table may be demonstrated by an example:

Given: Shell roof (e.g. Rapid City - Hangar)

Scale factor n = 30

Wind pressure p = 140.62 lb/in. ($p_{Mod} = p_{Orig}$)

To find: Fiber stresses σ_u, σ_L of the rib at the springing line (σ_u is the max. stress occurring in the ribs).

Solution: Model: σ_u = 17666.3 lb/in²

σ_L = 1168.8 "   (From Table III)

δ = -8.525 $\cdot$ 10⁻² in. (From page 16)

Shell roof: $\sigma_{Orig} = \frac{1}{n}$ $\sigma_{Mod} = \frac{1}{30} \sigma_{Mod}$

$$\sigma_u = 588.9 \text{ lb/in.}^2$$

$$\sigma_L = 39.0 \text{ lb/in.}^2$$

$$\delta_{Orig} = \frac{E_{Mod}}{E_{Orig}} \cdot \delta_{Mod} = 10 \, \delta_{Mod}$$

$$\delta = -0.853 \text{ in.}$$

The actual end wind pressure on a hangar of the "Rapid-City type" is 30 to 35 lb/ft², or approximately 1000 lb/per ft. of arch length. If this load is applied to a shell roof in scale 30:1 of the tested model, then:

$$p = 1000 \text{ lb/ft.} = 85 \text{ lb/in.:}$$

$$\sigma_u = 356 \text{ lb/in.}^2$$

The meaning of this result is, that one shell-unit of the whole shell-roof is able to carry a horizontal wind-pressure of about 1000 lb/ft. arch length under a maximum rib stress of $\sigma_u = 356 \text{ lb/in.}^2$ The action of the entire shell, composed of a number of units, decreases this stress considerably.

Conclusions

The present investigation has resulted in a method for the analysis of shell-roof constructions under end loads (primarily wind). The analysis has been verified by tests performed on a model.

TABLE I

Base System

Normal force N_O, bending moment M_O, (Eq. (5) and (6)

$$(1 - \frac{y_s}{R_e}) \frac{1}{2} = 0.4960\ 20 \qquad A_1 = \frac{R_s^2}{h}\ p = 6.8927 \cdot 10^4 \qquad A_2 = \frac{R_s^2}{h}\ pR_e = 7.5080 \cdot 10^6$$

①	②	③	④	⑤	⑥	⑦	⑧
ω	ω^2	$\cos\omega$	$1-\cos\omega$	$(1-\frac{y_s}{R_e})\frac{\omega^2}{2}$	⑤-④	$N_O = A_1$④	$M_O = -A_2$⑥
0.	0.	1.	0.	0.	0.	0.	0.
0.0580	0.0033 59	0.9983 18	0.0016 82	0.0016 66	-0.0000 16	115.94	120.13
0.1159	0.0134 33	0.9932 91	0.0067 09	0.0066 63	-0.0000 46	462.43	345.37
0.1739	0.0302 35	0.9849 17	0.0150 83	0.0149 97	-0.0000 86	1039.62	645.69
0.2319	0.0537 78	0.9732 31	0.0267 69	0.0266 75	-0.0000 94	1845.11	705.75
0.2898	0.0839 85	0.9583 01	0.0416 99	0.0416 58	-0.0000 41	2874.19	307.83
0.3478	0.1209 65	0.9401 25	0.0598 75	0.0600 01	+0.0001 26	4127.00	- 946.01
0.4057	0.1645 92	0.9188 26	0.0811 74	0.0816 41	+0.0004 67	5595.08	- 3506.24
0.4637	0.2150 18	0.8944 04	0.1055 96	0.1066 53	+0.0010 57	7278.42	- 7935.96
0.5216	0.2721 11	0.8670 23	0.1329 77	0.1349 72	+0.0019 95	9165.71	-14978.46
0.5796	0.3359 36	0.8366 82	0.1633 18	0.1666 31	+0.0033 13	11257.02	-24874.00
0.5866	0.3441 00	0.8328 28	0.1671 72	0.1706 80	+0.0035 08	11522.66	-26338.06

TABLE II

a. Fully Restrained Rib:

N, M and fiber-stresses σ_u, σ_L

$$H_c = 1068.1 \text{ lb.} \qquad \frac{y_u}{I} = 2.2145$$

$$M_c = 3155.9 \text{ in-lb} \qquad \frac{y_L}{I} = 1.7287$$

$$H_c R_e = 1.1634 \cdot 10^5 \qquad \frac{1}{A} = 0.8149$$

⑨	⑩	⑪	⑫	⑬	⑭	⑮	⑯	⑰	⑱
ω	$H_c \cos\omega$	$H_c R_e$④	N=⑦-⑩	M=M_c+⑧+⑪	$\frac{N}{A}$	$M\frac{y_u}{I}$	$M\frac{y_L}{I}$	σ_u=⑭-⑮	σ_L=⑭+⑯
0.	1068.1	0.	-1068.1	- 3155.9	-870.4	-6988.7	-5455.6	6118.3	-6326.0
0.0580	1066.3	195.7	- 950.4	- 2840.1	-774.5	-6289.4	-4909.7	5514.9	-5684.2
0.1159	1060.8	780.5	- 598.4	- 2030.0	-487.6	-4495.4	-3509.3	4007.8	-3996.9
0.1739	1052.0	1754.8	- 12.4	- 755.4	- 10.1	-1672.8	-1305.9	1662.7	-1316.0
0.2319	1039.5	3114.4	805.6	664.3	656.5	1471.1	1148.4	- 814.6	1804.9
0.2898	1023.6	4851.4	1850.6	2003.3	1508.1	4436.3	3463.1	-2928.2	4971.2
0.3478	1004.1	6965.3	3122.9	2863.4	2544.9	6341.0	4950.0	-3796.1	7494.9
0.4057	981.4	9443.9	4613.7	2781.8	3759.7	6160.3	4808.9	-2400.6	8568.6
0.4637	955.3	12285.0	6323.1	1193.1	5152.7	2642.1	2062.5	2510.6	7215.2
0.5216	926.0	15470.5	8239.7	-2663.9	6714.5	-5899.2	-4605.1	12613.7	2109.4
0.5796	893.6	19000.4	10363.4	- 9029.5	8445.1	-19995.8	-15609.3	28440.9	-7164.2
0.5866	889.5	19448.8	10633.2	-10045.2	8665.0	-22245.1	-17365.1	30910.1	-8700.1

TABLE III

b. Elastically Restrained Rib:

N, M and fiber-stresses σ_u, σ_L

$$H_c = 1456.7 \; lb \qquad\qquad \frac{y_u}{I} = 2.2145$$

$$M_c = -4370.6 \; in\text{-}lb \qquad \frac{y_L}{I} = 1.7287$$

$$H_c R_e = 1.5867 \cdot 10^5 \qquad\qquad \frac{1}{A} = 0.8149$$

⑲	⑳	㉑	㉒	㉓	㉔	㉕	㉖	㉗	㉘
ω	$H_c \cos\omega$	$H_c R_e \textcircled{4}$	$N=⑦-⑳$	$M=M_c+⑧+㉑$	$\frac{N}{A}$	$M\frac{y_u}{I}$	$M\frac{y_u}{I}$	σ_u	σ_L
0.	1456.7	0.	-1456.7	-4370.6	-1187.1	-9678.7	-7555.5	8491.6	-8742.6
0.0580	1454.2	266.9	-1338.3	-3983.6	-1090.6	-8821.7	-6886.4	7731.1	-7977.0
0.1159	1446.9	1064.5	-984.5	-2960.7	-802.3	-6556.5	-5118.2	5754.2	-5920.5
0.1739	1434.7	2393.2	-395.1	-1331.7	-322.0	-2949.0	-2302.1	2627.0	-2624.1
0.2319	1417.7	4247.4	427.4	582.6	348.3	1290.2	1007.1	-941.9	1355.4
0.2898	1396.0	6616.5	1478.2	2553.7	1204.6	5655.2	4414.6	-4450.6	5619.2
0.3478	1369.4	9500.4	2757.6	4183.8	2247.2	9265.0	7232.5	-7017.8	9479.7
0.4057	1338.4	12879.9	4256.7	5003.1	3468.8	11079.4	8648.9	-7610.6	12117.7
0.4637	1302.9	16755.6	5975.5	4449.0	4869.4	9852.3	7691.0	-4982.9	12560.4
0.5216	1263.0	21100.0	7902.7	1750.9	6439.9	3877.4	3026.8	2562.5	9466.7
0.5796	1218.8	25914.0	10038.2	-3330.6	8180.1	-7375.6	-5757.6	15555.7	2422.5
0.5866 **	1213.1	26524.9	10309.6	-4183.8	8401.3	-9265.0	-7232.5	17666.3	1168.8

TABLE IV

Deflection of the Ribs

Elastically restrained ribs (M and H from Table III)

$$\frac{R_\Theta}{2} = 54.463$$

①	②	③	④	⑤	⑥	⑦	⑧	⑨	⑩	⑪
ω	$\sin\omega$	$\sin\omega_k - \sin\omega$	$M'=\frac{R_\Theta}{2}$ ③	$N'=-\frac{1}{2}$②	M Table III	N Table III	M'M	N'N	$\frac{1}{2}$M'M	$\frac{1}{2}$N'N
0.	0.	0.5535	30.145	0.	-4370.6	-1456.7	-13.175	0.	-6.588	0.
0.0580	0.0578	0.4957	26.997	-0.0289	-3983.6	-1338.3	-10.755	0.387		
0.1159	0.1156	0.4379	23.849	-0.0579	-2960.7	- 984.5	- 7.061	0.569		
0.1739	0.1730	0.3805	20.723	-0.0865	-1331.7	- 395.1	- 2.760	0.342		
0.2319	0.2298	0.3237	17.630	-0.1149	582.6	427.4	1.027	-0.491		
0.2898	0.2858	0.2677	14.580	-0.1429	2553.7	1478.2	3.723	-2.112		
0.3478	0.3408	0.2127	11.584	-0.1704	4183.8	2757.6	4.847	-4.699		
0.4057	0.3947	0.1588	8.649	-0.1973	5003.1	4256.7	4.327	-8.398		
0.4637	0.4473	0.1062	5.784	-0.2236	4449.0	5975.5	2.573	-13.361		
0.5216	0.4983	0.0552	3.006	-0.2491	1750.9	7902.7	0.526	-19.686		
0.5796	0.5477	0.0058	0.316	-0.2738	-3330.6	10038.2	-0.105	-27.485	-0.052	-13.742
0.5866	0.5535	0.	0.	-0.2768	-4183.8	10309.6	0.	-28.537	0.	-14.268

Multiplier $.10^4$ $.10^2$

		ΣM'M	ΣN'N	Δs
Integration: ω = 0 to 0.5796	1.)	-10.193	-61.191	6.318
ω = 0.5796 to 0.5866	2.)	- 0.052	-28.010	0.762

TABLE V

Shell:

String Force Y and Direct Force $T_2|_{x=0}$

(Elastically restrained ribs)

$$d = 0.118 \qquad b = 1.356$$

①	②	③	④	⑤	⑥	⑦	⑧
ω	σ_L Table III	σ_u Table III	$\sigma_L - \sigma_u$	$0.028 \cdot$ ④	$\sigma_s=$②-⑤	$T_2\big|_{x=0}$ = d·⑥	Y=b · ⑦
0.	-8742.6	8491.6	-17485.2	-489.6	-8253.0	-973.9	-1320.6
0.0580	-7977.0	7731.1	-15708.1	-439.8	-7537.2	-889.4	-1206.0
0.1159	-5920.5	5754.2	-11674.7	-326.9	-5593.6	-660.0	-895.0
0.1739	-2624.1	2627.0	-5251.1	-147.0	-2477.1	-292.3	-396.4
0.2319	1355.4	-941.9	2297.3	64.3	1291.1	152.3	206.6
0.2898	5619.2	-4450.6	10069.8	281.9	5337.3	629.8	854.0
0.3478	9479.7	-7017.8	16497.5	461.9	9017.8	1064.1	1442.9
0.4057	12117.7	-7610.6	19728.3	552.4	11565.3	1364.7	1850.6
0.4637	12560.4	-4982.9	17543.3	491.2	12069.2	1424.2	1931.2

TABLE VI

Shell:

Forces T_2 (lb/in) and Moments M_1 (in-lb/in)

	x=0"	1"	2"	3"	4.5"	6"	9"	12"	

1.) T_2 due to $Y = 1$ (Table IV, Progress Report 213-B)

	x=0"	1"	2"	3"	4.5"	6"	9"	12"	
	73.72	47.56	26.11	10.93	-1.24	-4.83	-2.62	-0.25	
						-0.09	-0.21	0.25	
	73.72	47.56	26.11	10.93	-1.24	-4.92	-2.83	0	10^{-2}

2.) M_1 due to $Y = 1$

	x=0"	1"	2"	3"	4.5"	6"	9"	12"	
	0	626.1	808.0	742.9	476.2	220.3	-16.1	-28.9	
						-1.0	6.8	28.9	
	0	626.1	808.0	742.9	476.2	219.3	-9.3	0	10^{-5}

3.) Section $\omega = 0$: $Y = -1320.6$ lb

	x=0"	1"	2"	3"	4.5"	6"	9"	12"	
T_2	-973.5	-628.1	-344.8	-144.3	16.4	65.0	37.4	0	lb/in
M_1	0	-8.268	-10.670	-9.979	-6.289	-2.896	0.123	0	in-lb/in

4.) Section $\omega = 0.058$: $Y = -1206.0$ lb

	x=0"	1"	2"	3"	4.5"	6"	9"	12"	
T_2	-889.1	-673.6	-314.9	-131.8	15.0	59.3	34.1	0	lb/in
M_1	0	-7.551	-9.744	-8.959	-5.743	-2.645	0.112	0	in-lb/in

5.) Section $\omega = 0.1739$: $Y = -396.4$ lb

	x=0"	1"	2"	3"	4.5"	6"	9"	12"	
T_2	-292.2	-188.5	-103.5	-43.3	4.9	19.5	11.2	0	lb/in
M_1	0	-2.482	-3.203	-2.945	-1.888	-0.650	0.037	0	in-lb/in

TABLE VI (continuation)

6.) Section $\omega = 0.2898$: Y = 854.0 lb

T_2	629.6	406.2	223.0	93.3	-10.6	-42.0	-24.2	0	lb/in
M_1	0	5.347	6.900	6.344	4.067	1.873	-0.079	0	in-lb/in

7.) Section $\omega = 0.4057$: Y = 1850.6 lb

T_2	1364.3	880.1	483.2	202.3	-22.9	-91.0	-52.4	0	lb/in
M_1	0	11.587	14.953	13.748	8.813	4.058	-0.172	0	in-lb/in

8.) Section $\omega = 0.4637$: Y = 1931.2 lb

T_2	1423.7	918.5	504.2	211.1	-23.9	-95.0	-54.7	0	lb/in
M_1	0	12.091	15.604	14.347	9.196	4.235	-0.180	0	in-lb/in

FRONT VIEW 1" = 10"

SHELL ROOF MODEL
SHOWING MEASURED
DIMENSIONS.

ALL DIMENSIONS IN
INCHES

0.118

R = 108"

59.78   59.78

TOP VIEW 1" = 10"

10.85   11.35   11.72   11.93   6

1.0
2.0   3.75

SECTION C-C   1" = 4"

0.505   0.625   0.505

0.118   2.113

SECTION A-A
1" = 4"

2.0   6.0   2.113

0.20

0.118

1.0

2.5   0.86   0.257   0.257

3.5   1.0   0.5   2.25   1.0

1.5

10.0

SECTION B-B
1" = 4"

12.0   12.0

0.505   0.625   0.505

0.118

3.5

1.0   1.0   1.0

3.5

1.5

3.0   12.0   12.0   3.0
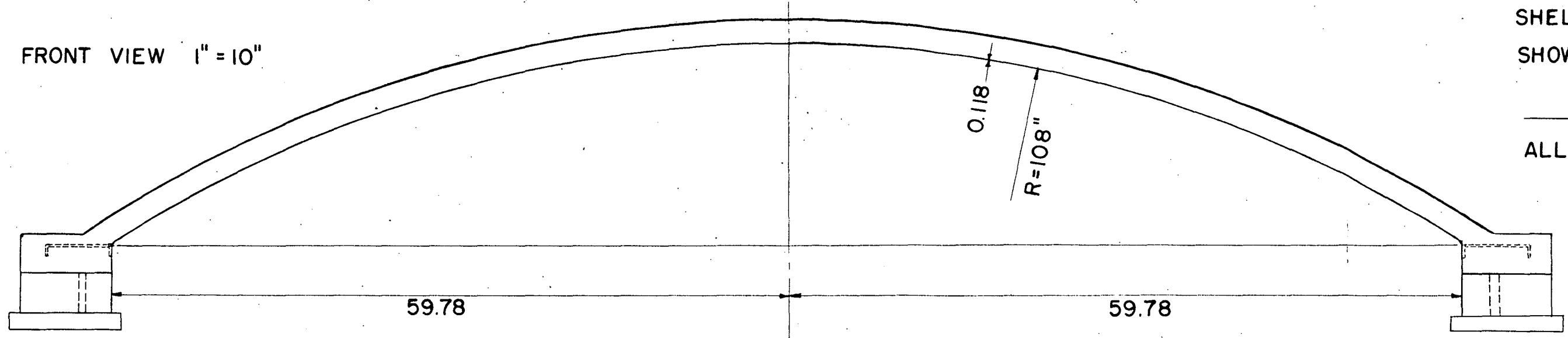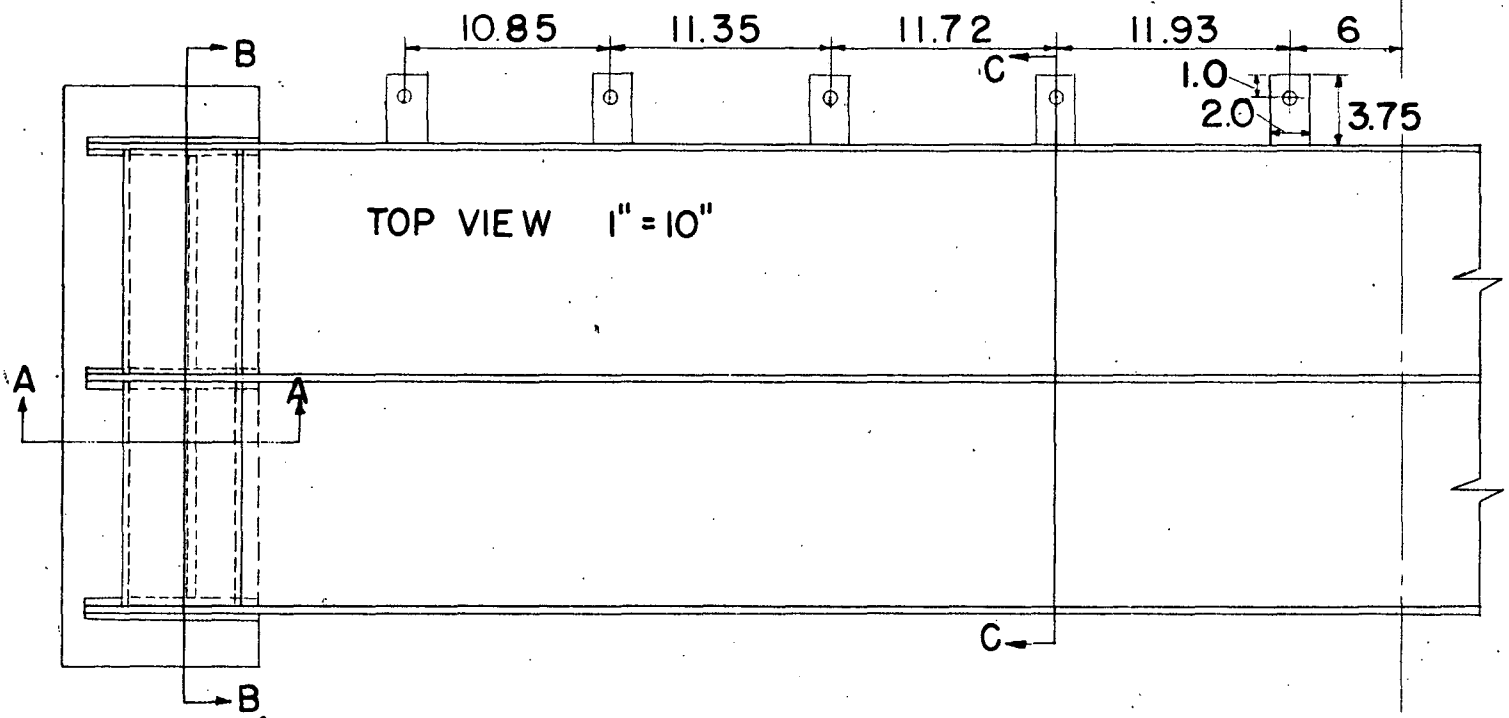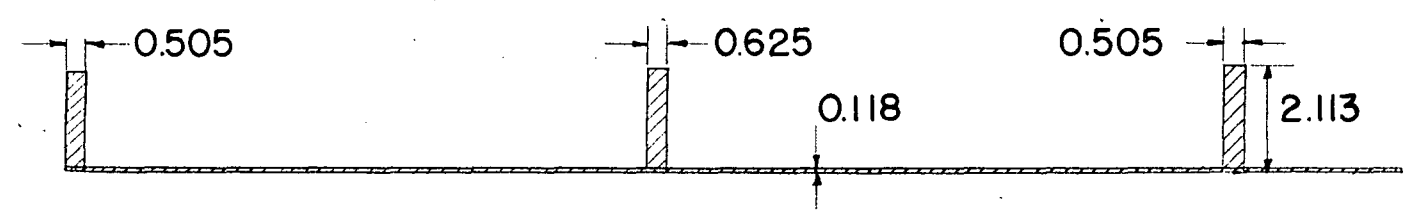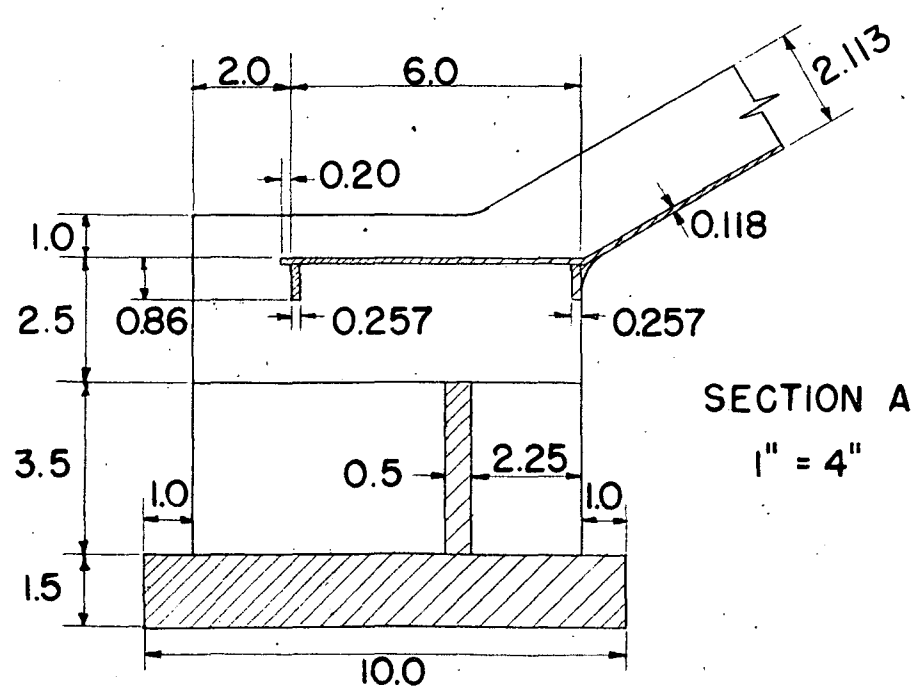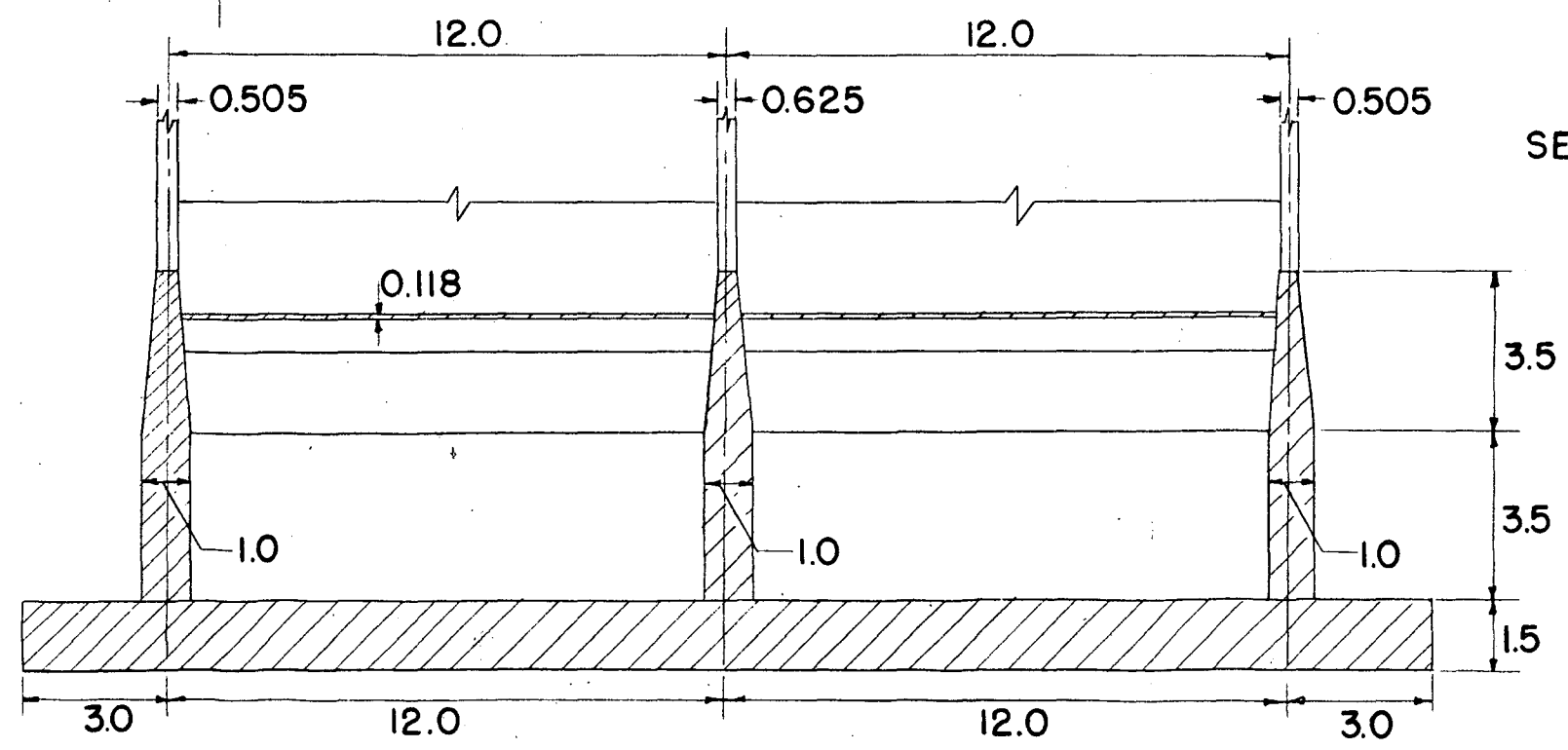
FIG. 1

a. Uniform lateral load (Test and Analysis)

Assumption in theoretical analysis

$p = 140.62\,lb/in$

Actual loading in test
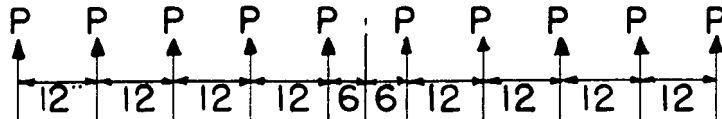
$P = 1687.5\,lb$
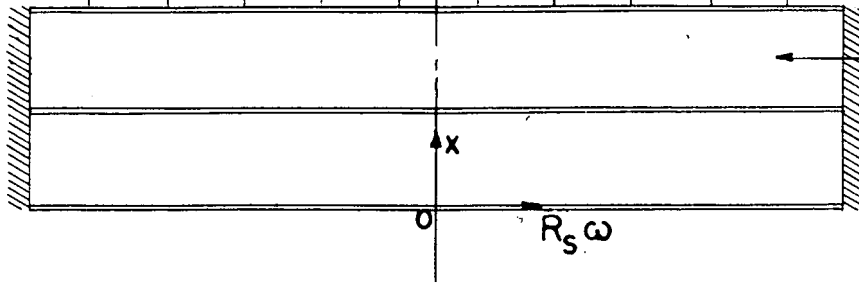
Developed shell surface

Edge member

b. Lateral loads at center (Test)

Actual loading in test.
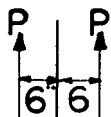
$P = 3187.5\,lb$
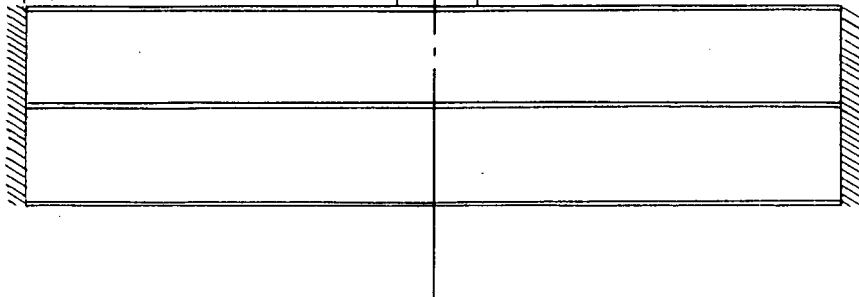
c. Lateral load at quarter-point (Test)

Actual loading in test.
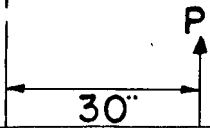
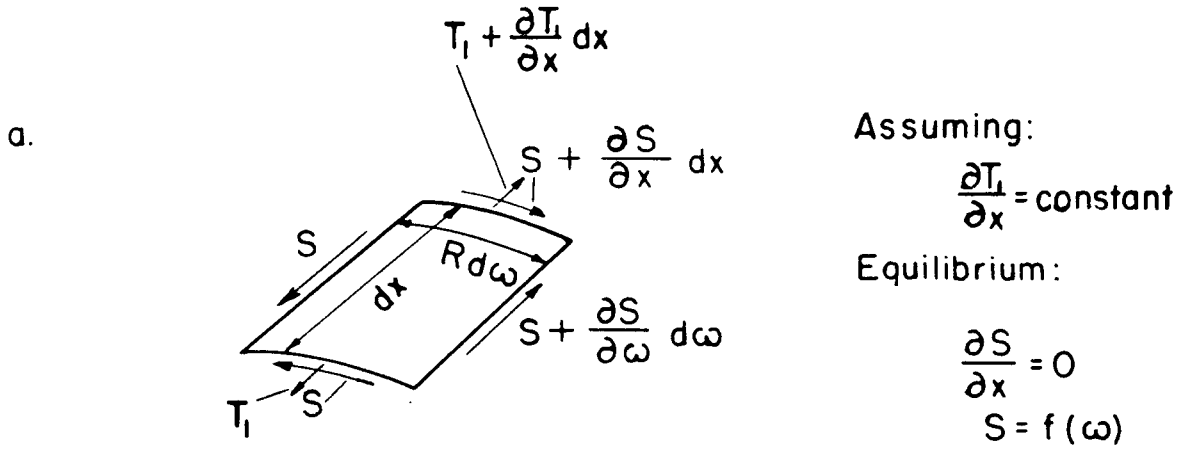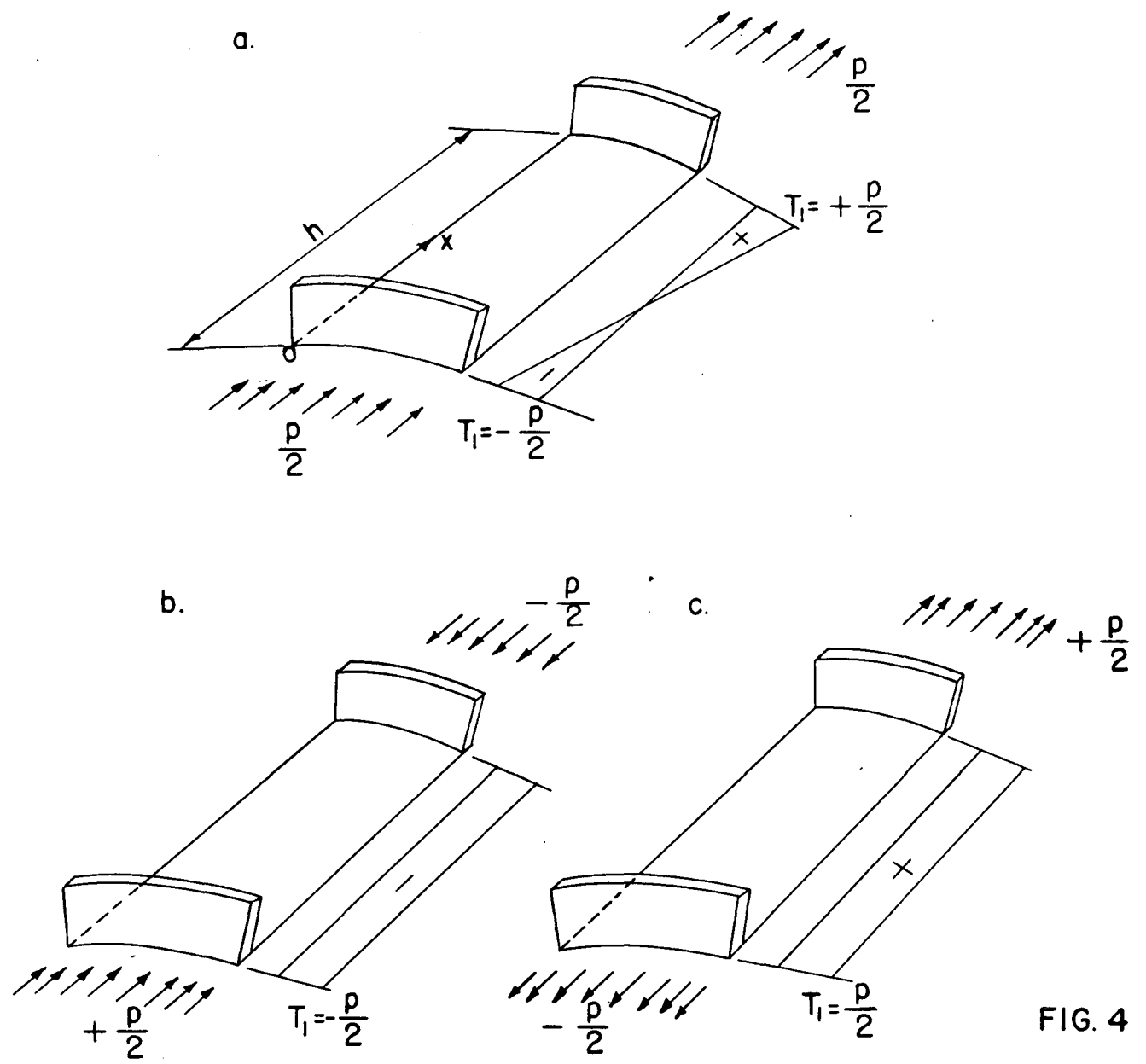$P = 5647.5\,lb$
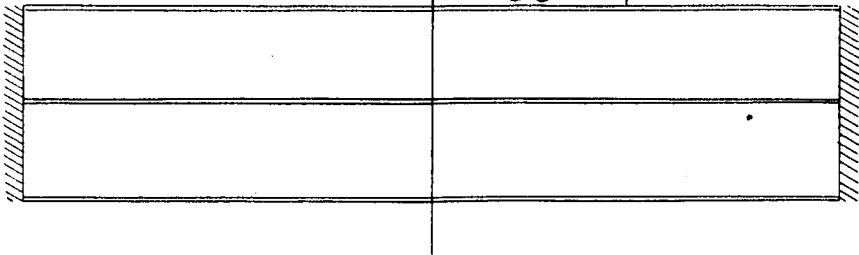
Investigation of 3 cases of lateral loads

FIG. 2

a.

$T_l + \dfrac{\partial T_l}{\partial x}\,dx$

$S + \dfrac{\partial S}{\partial x}\,dx$

S

$R\,d\omega$

dx

$S + \dfrac{\partial S}{\partial \omega}\,d\omega$

T_l S

Assuming:

$$\frac{\partial T_l}{\partial x} = \text{constant}$$

Equilibrium:

$$\frac{\partial S}{\partial x} = 0$$

$$S = f(\omega)$$

b.

x

S

S

h S

$S + \dfrac{\partial S}{\partial \omega}\,d\omega$

S S

$R_s\omega$

p R_s

$d\omega$

Equilibrium:

$$h \cdot \frac{\partial S}{\partial \omega}\,d\omega + pR\,d\omega = 0$$

$$\frac{\partial S}{\partial \omega} = -\frac{R_s}{h}\,p$$

c. Displacements:

x

u

v

$R_s\omega$

w

FIG. 3

a.

h

x

o

$\frac{p}{2}$

$T_l = +\frac{p}{2}$

$+$

$T_l = -\frac{p}{2}$

$\frac{p}{2}$

b.

$-\frac{p}{2}$

$+\frac{p}{2}$

$T_l = -\frac{p}{2}$

$-$

c.

$+\frac{p}{2}$

$-\frac{p}{2}$

$T_l = \frac{p}{2}$

$+$
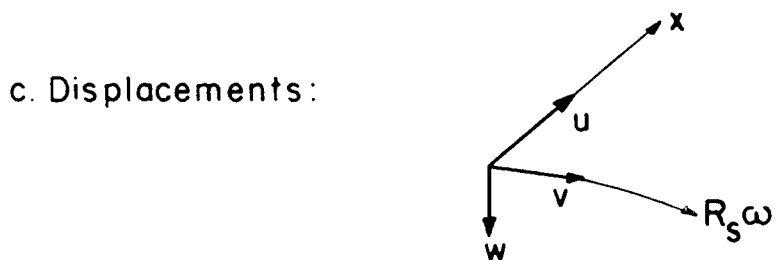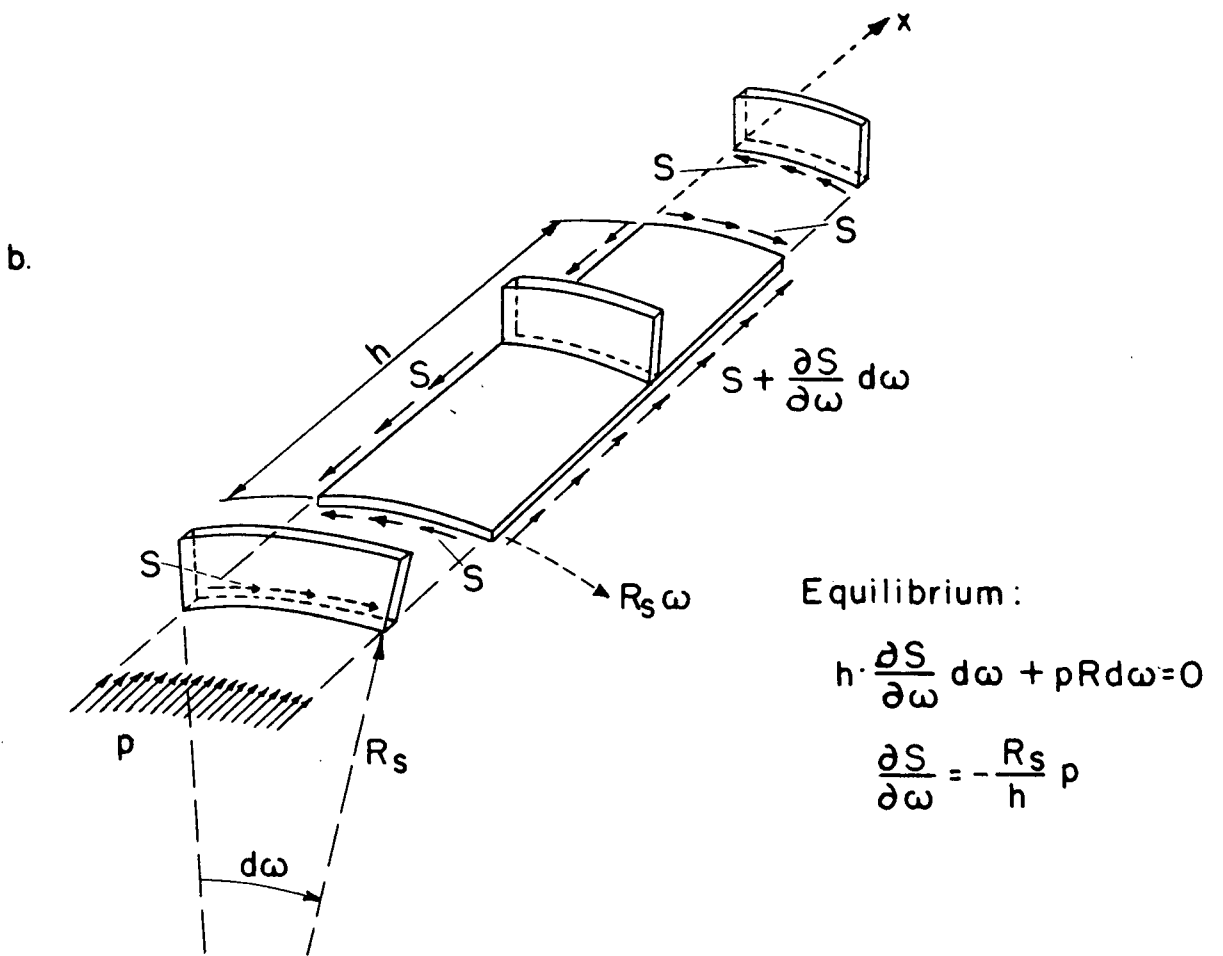
FIG. 4

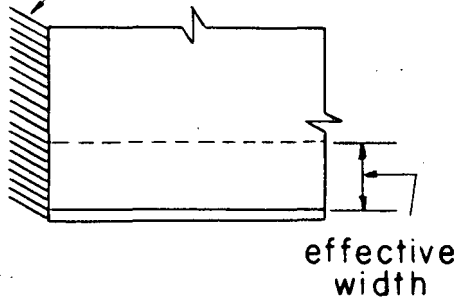a + b ⟶ Compression p at x = 0   a + c ⟶ Tension p at x = h

a.

$Rd\omega$

$-S$

y

b.

$b = $ effective width

S

FIG. 5

a.

rib

shell

edge member

end wall
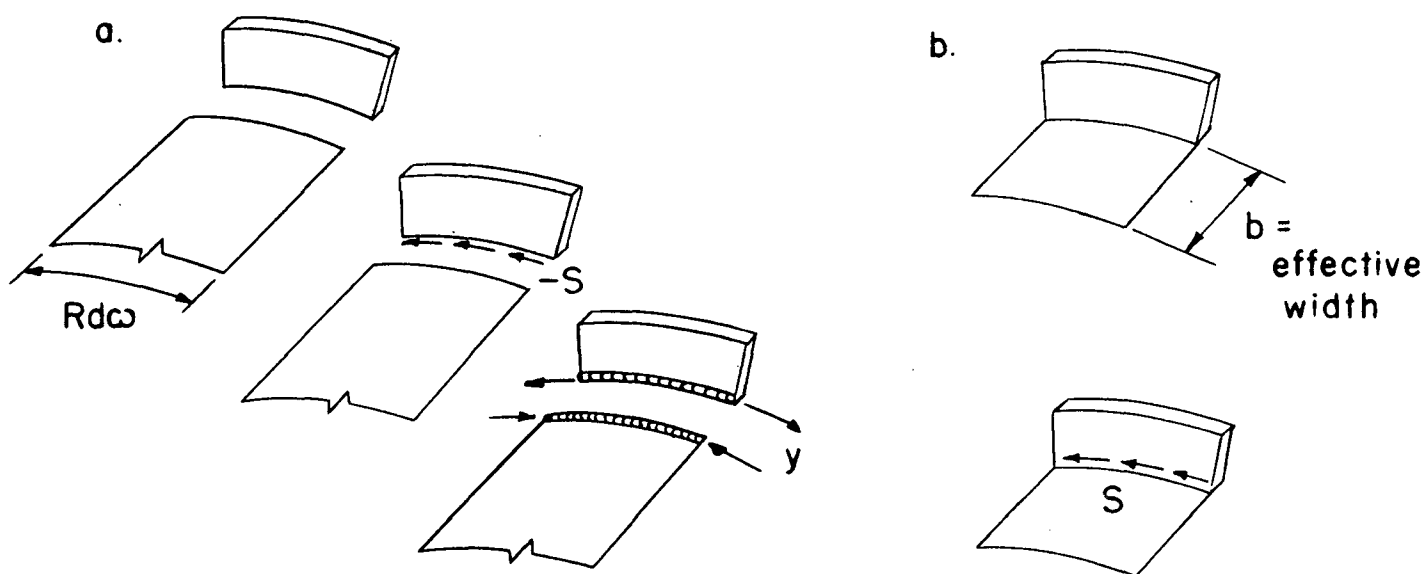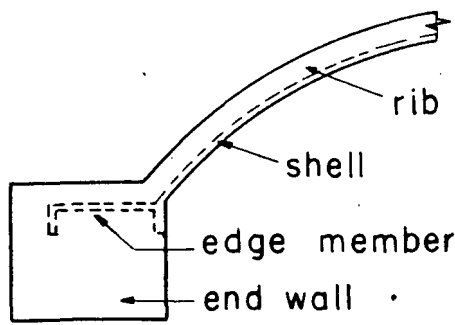
Actual support conditions

middle rib

edge member

shell

end wall

rib

b.

rigid support

rigid support

rigid support

c.

rigid support

FIG.6

free edge

zone of disturbance

effective width

rigid support

effective width
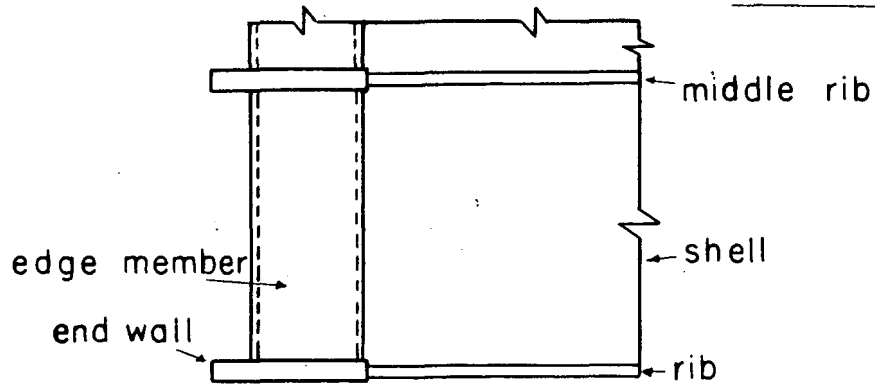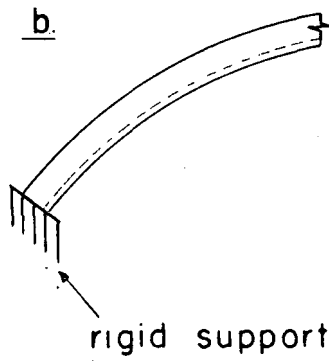
Case 1: Fully rigid support
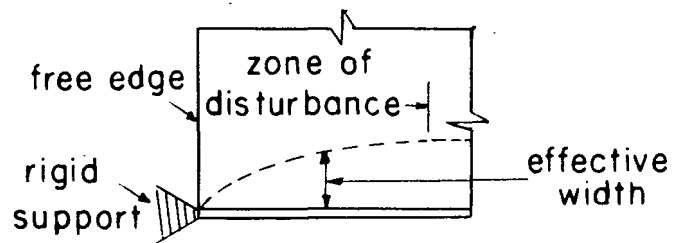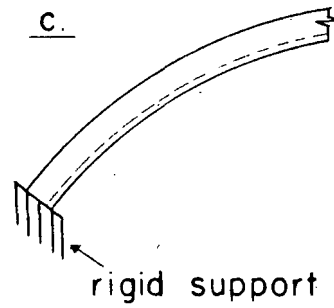
Case 2: Rigid support of rib
No support of edge member

middle line of rib

$M_k = -1$

support

M_k

κ

$\varphi_k = -\kappa \cdot M_k$

FIG.7

a.

y_s = distance between centroid of effective section and center plane of shell.

M_C

H_C

y_s

R_e R_s

ω

ω_k

b.

$(\omega-\alpha)\,R_e\left[1-\cos(\omega-\alpha)\right]$

y_s

$SR_s d\alpha$

N

M

$y_s - R_e\left[1-\cos(\omega-\alpha)\right]$

α

$(\omega-\alpha)$

$d\alpha$

ω

c.

$R_e(\cos\omega - \cos\omega_k)$

$P=1$

ω

ω_k

R_e

displacement δ_k

d.

$M=1$

FIG. 8

M, N

S

$P=1$

M', N'

Actual structure:

    Elastically restrained arch

Actual load:

    Forces S

Virtual structure:

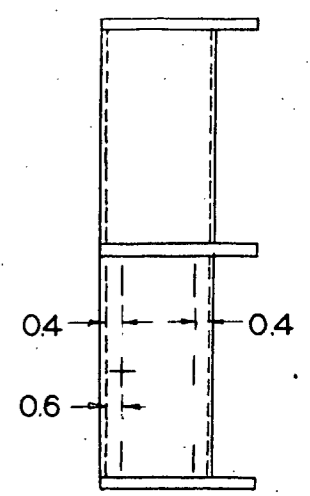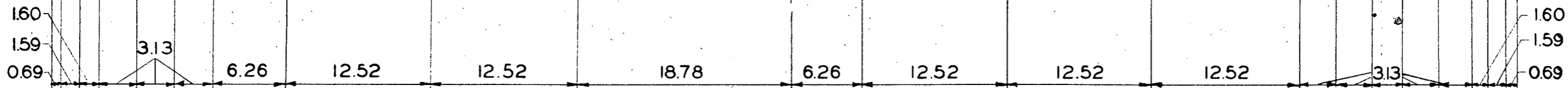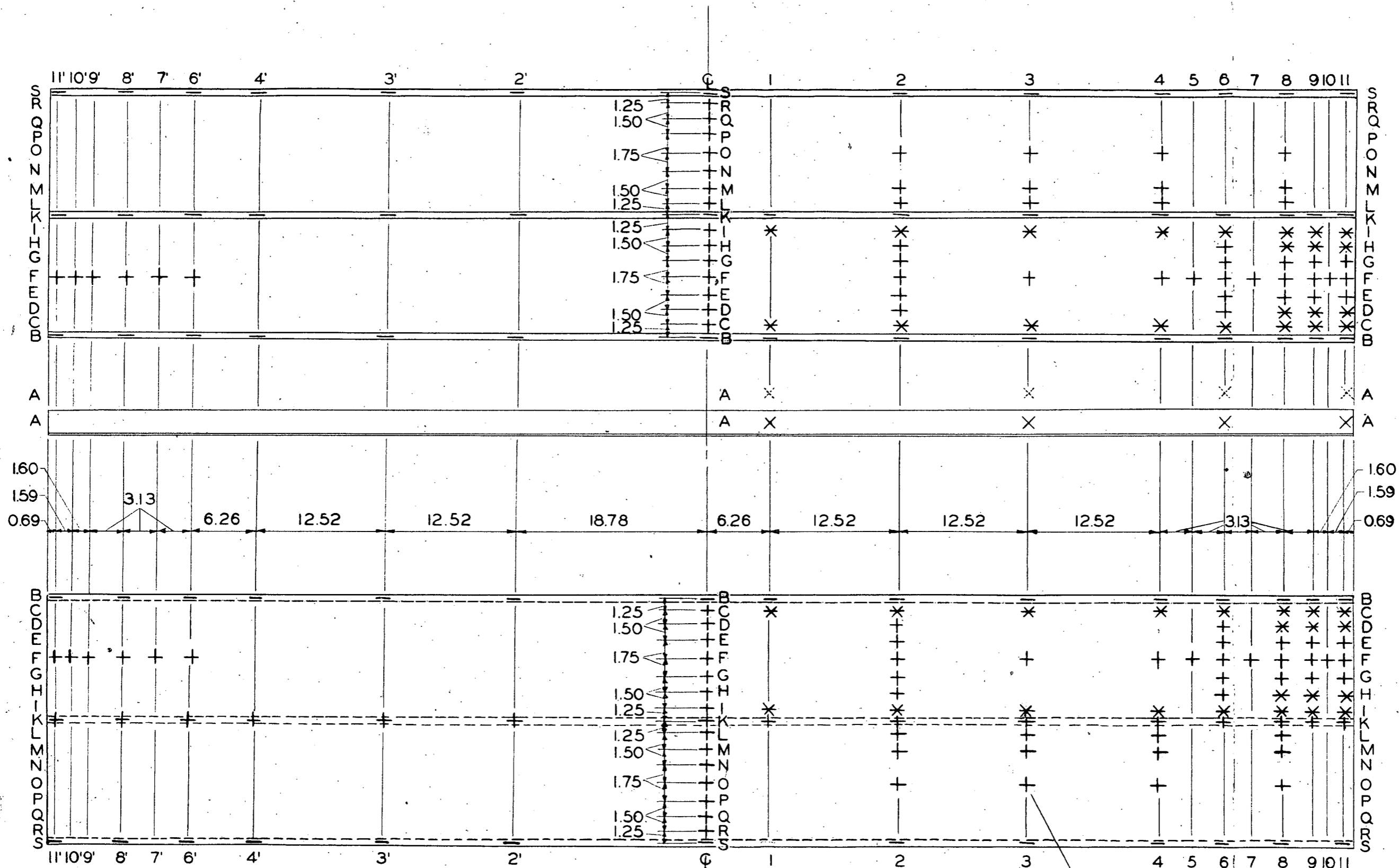   Simple beam

Virtual load:

    P=1
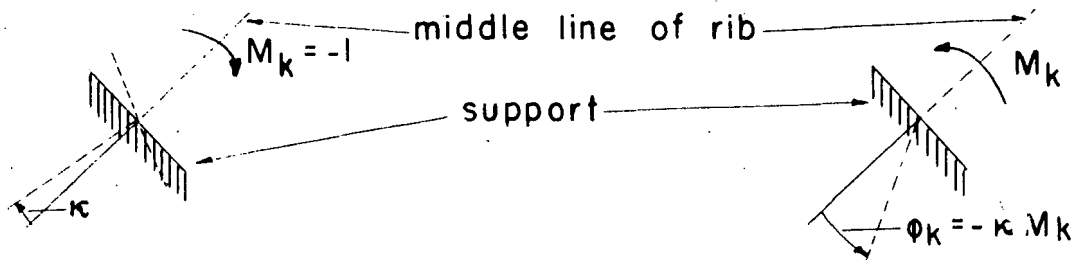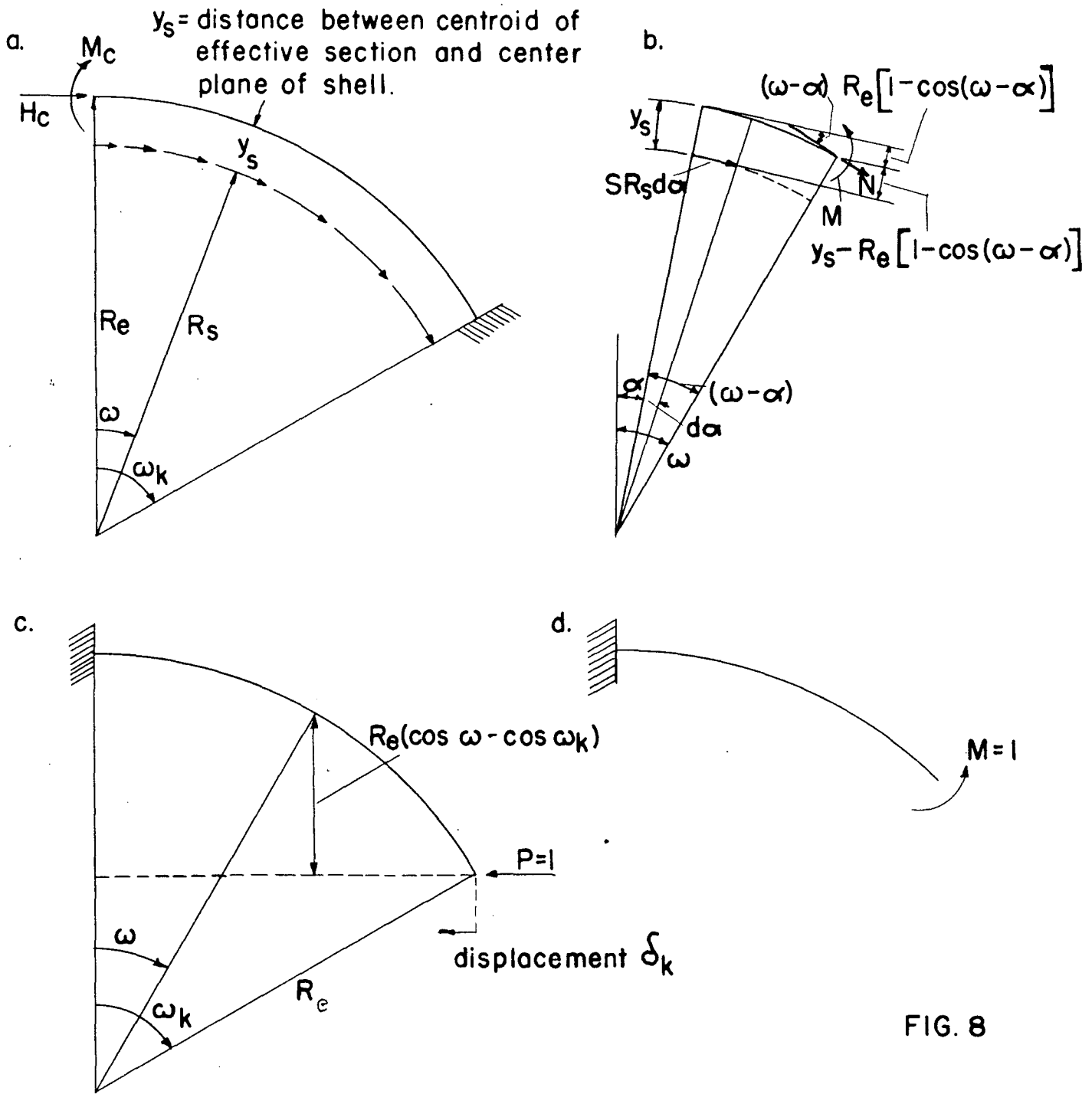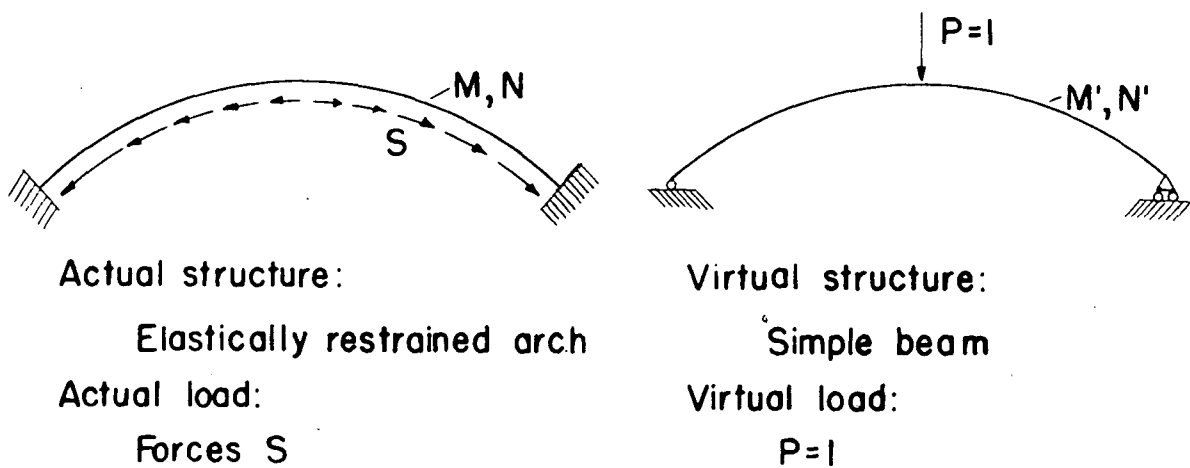
FIG. 9
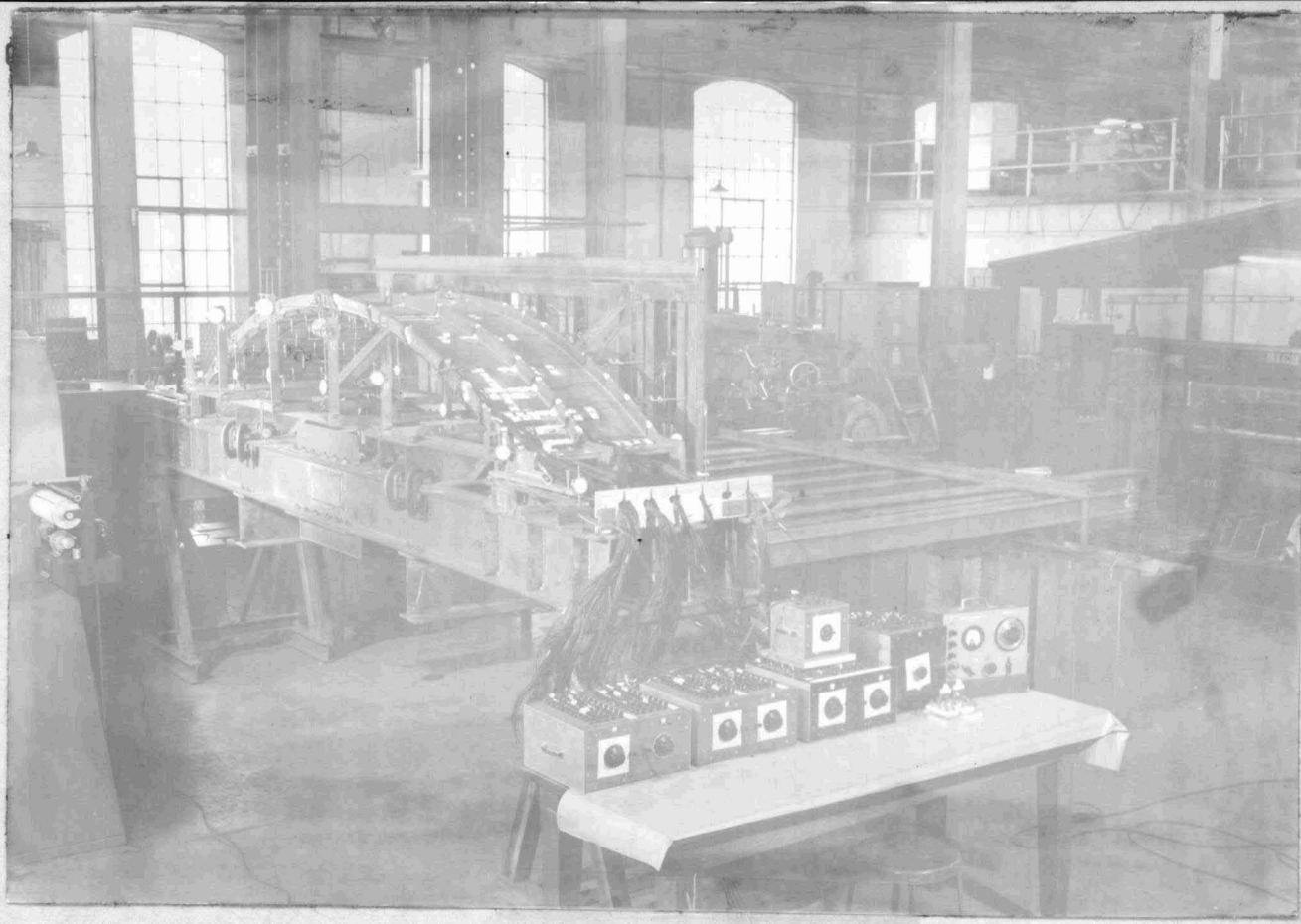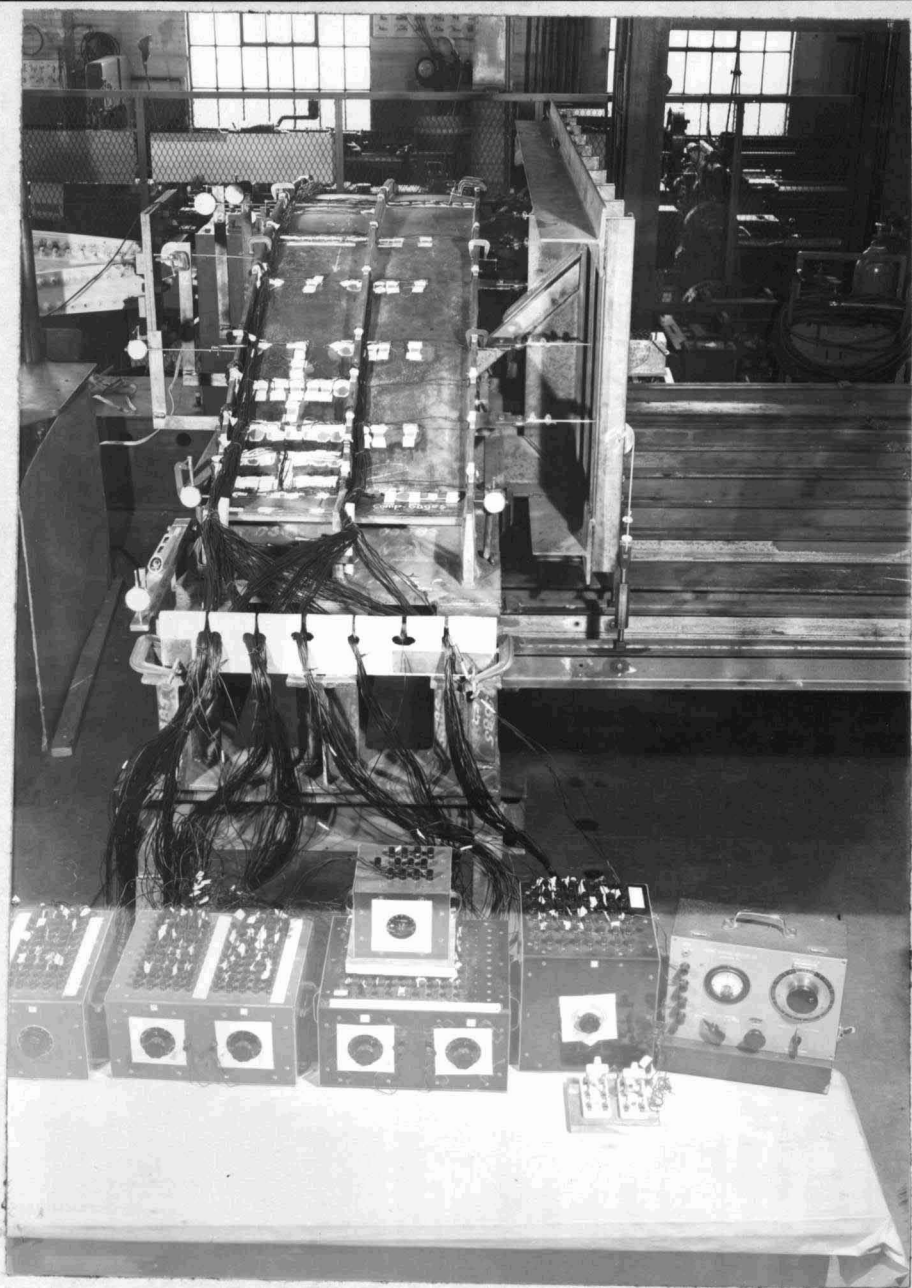
FIG. 10a

FIG. 10b
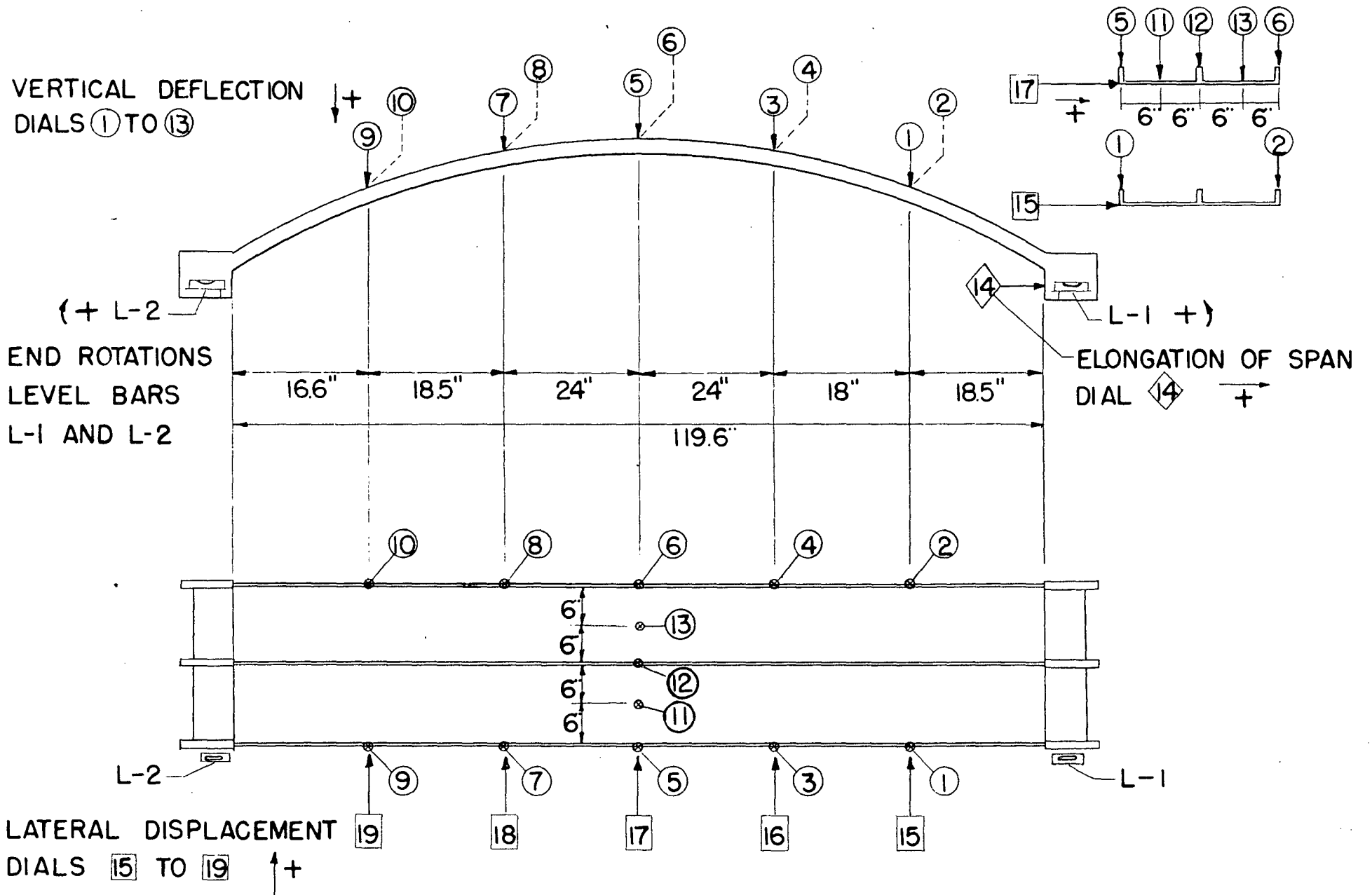
FIG. 10c
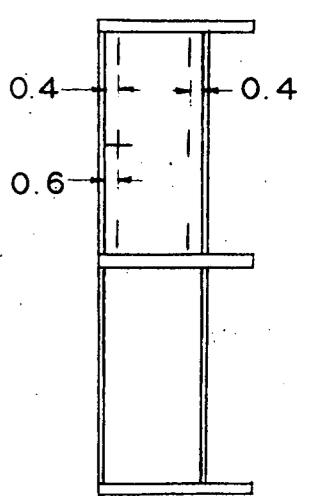
For example, this is gage O3

— Single gage
+ Cross gage
✳ Rosette gage

LAY-OUT OF STRAIN
GAGE COORDINATE
SYSTEM.   FIG. II

VERTICAL DEFLECTION
DIALS ① TO ⑬

(+ L-2

END ROTATIONS
LEVEL BARS
L-1 AND L-2

16.6" 18.5" 24" 24" 18" 18.5"

119.6"

L-1 +)

ELONGATION OF SPAN
DIAL ◇14◇ +

6" 6" 6" 6" 6" 6"

L-2

L-1

LATERAL DISPLACEMENT
DIALS ⑮ TO ⑲ ↑+

LAY-OUT OF DIAL GAGES AND LEVEL BARS

FIG. 12

FIBER-STRESS $(\frac{N}{A} \pm \frac{My}{I})$ AT UPPER AND LOWER EDGES OF RIBS.
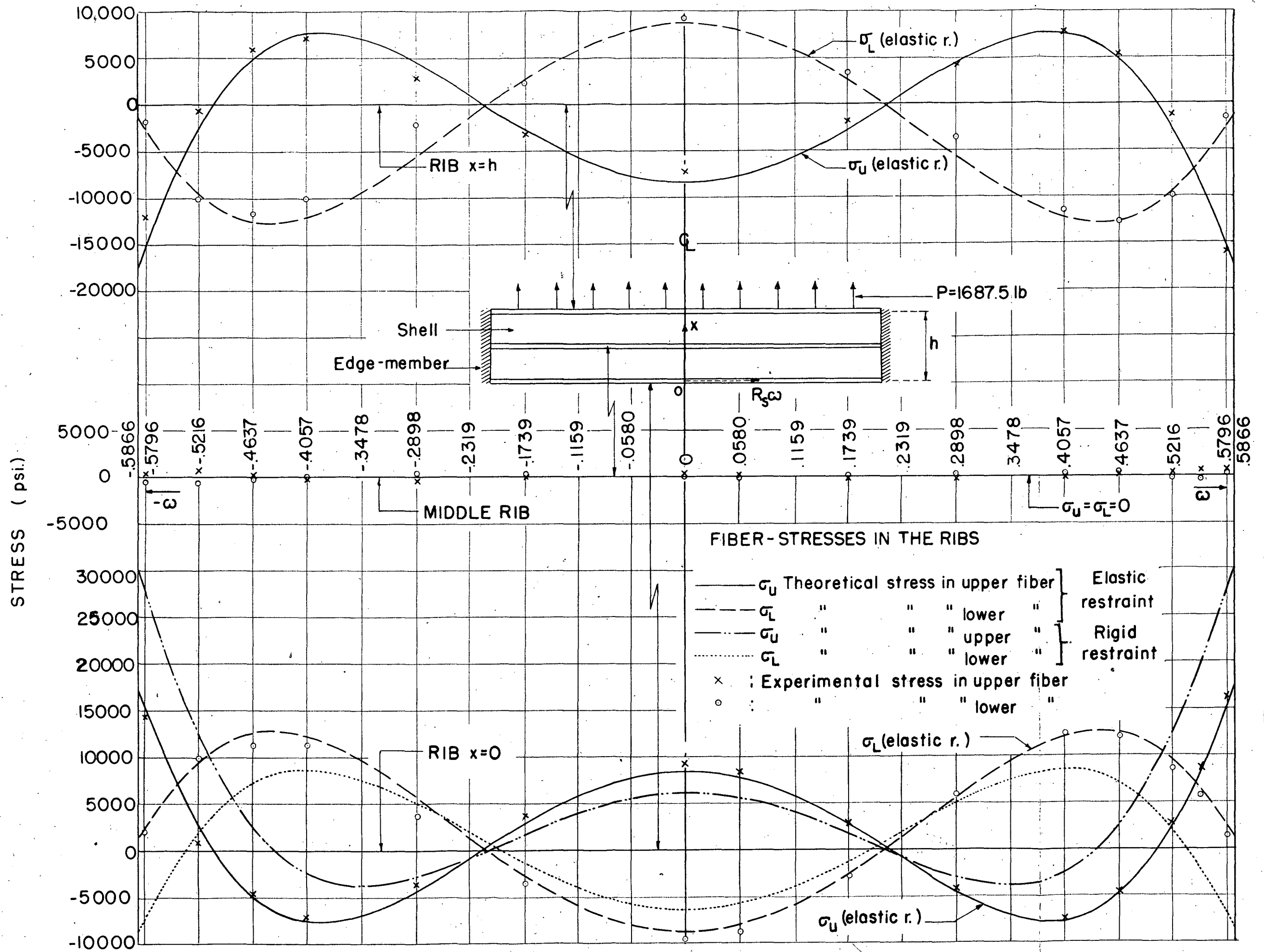
FIG. 13
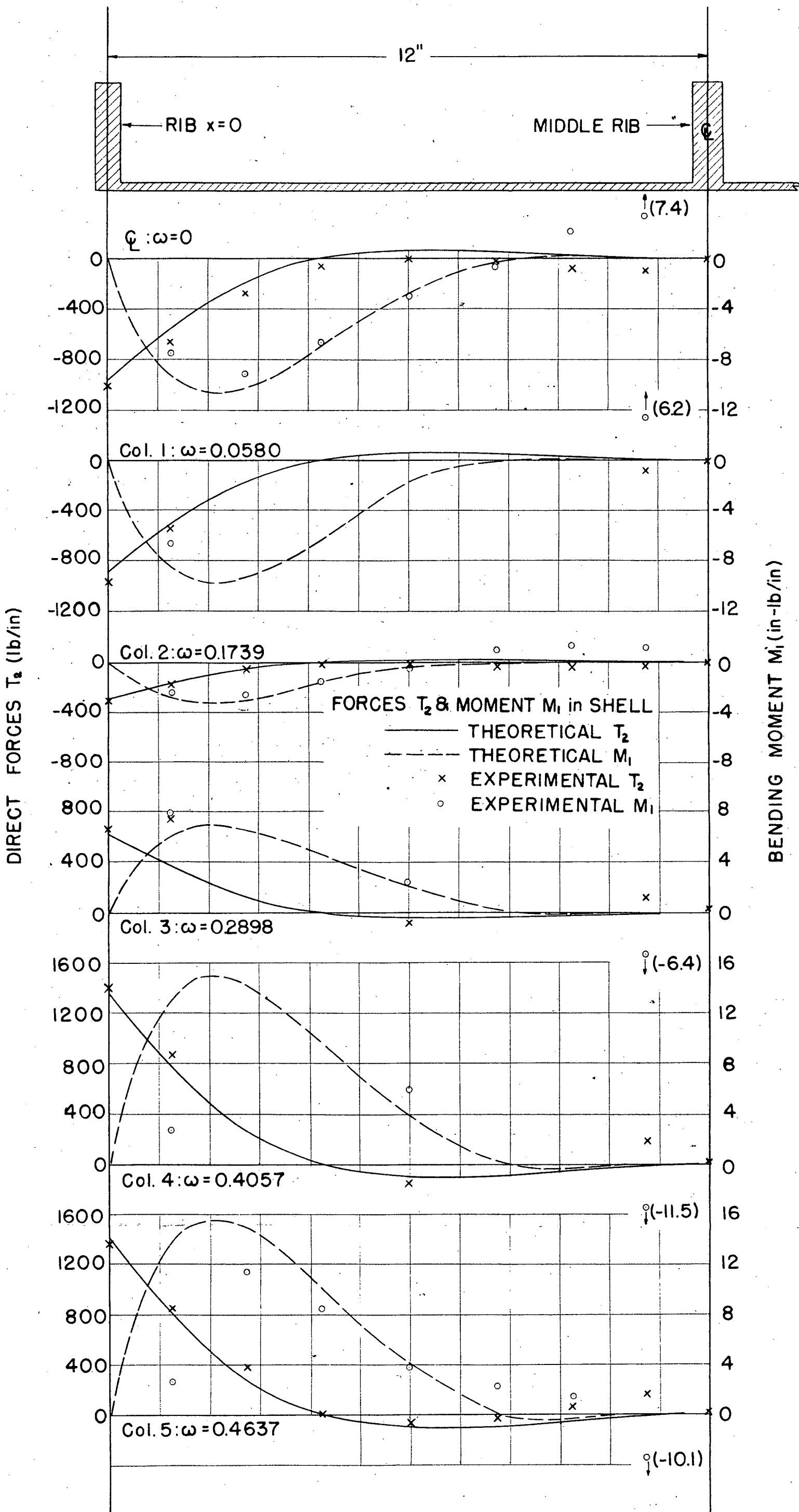
FIG. 14.

FORCES T₂ AND MOMENT M₁ IN SHELL.

DIRECT FORCES T₂ (lb/in)

BENDING MOMENT M₁ (in-lb/in)

NOTATIONS

Subscripts

S   refers to Shell

R   refers to Rib

u   refers to upper fiber of rib

L   refers to lower fiber of rib

Roman Alphabet

A, A_1, A_2 cross section area

b_R width of rib

$c = \dfrac{\pi}{2\omega_k}$ coefficient as given in Progress Report 213-B

d thickness of shell

E Modulus of elasticity

h distance between the two outer ribs = depth of the shell, Fig. 3

h_R height of the rib

I moment of inertia

K coefficient determining effective width b, see Progress Report 213-B, Eq. (41), (42), and Fig. 8

M bending moment of the rib (effective section)

M_c bending moment of the rib at the center, $\omega = 0$

M_k bending moment of the rib at the springing line, $\omega = \omega_k$

M_o bending moment of the rib in the statically determinate base system

M_1 bending moment per unit width of the shell in axial direction

M' bending moment used in the work equation due to the virtual load system

N normal force of the rib (effective section)

N_o normal force of the rib in the statically determinate base system

N' normal force used in the work equation due to the virtual load system

Q   statical moment of cross section

R_e radius of the effective section

R_S radius of the shell

R_R radius of the rib

S, S_{12}, S_{21} tangential shear forces per unit width of shell

T_1 normal force per unit width of shell in axial direction

T_2 normal force per unit width of shell in circumferential direction

u   displacement of shell in axial direction, Fig. 3

v   displacement of shell in circumferential direction, Fig. 3

w   displacement of shell in radial direction, Fig. 3

x   coordinate in axial direction, Fig. 3

Y   string force as given in Progress Report 213-B, p. 7 and Fig. 4

y_L distance between the lower fiber of the rib and the centroid of the effective section; see sketch p. 12

y_s distance between centroid of effective section and center plane of the shell, see sketch p. 12

y_u distance between the upper fiber of the rib and the centroid of the effective section; see sketch p. 12

Greek Alphabet

α angular coordinate, as used in Fig. 8b

β coefficient depending on shell dimensions, Progress Report 213B, Eq. (10) to (14)

δ deflection of the outer ribs at the center, $\omega = 0$

δ_k horizontal displacement of the abutment, Fig. 8c

κ coefficient of elastic restraint of the rib (effective section) by the abutment

$\lambda = c \sqrt{\dfrac{d}{R}}$ coefficient depending on shell dimensions and force distribution, Progress Report 213-B, p. 24

υ Poisson's ratio

σ_L stress in the lower fiber of the rib, see sketch p. 17

σ_s normal stress in rib in the fiber of the connecting line rib-shell, see sketch p. 17

σ_u stress in the upper fiber of the rib, see sketch p. 17

ω angular coordinate in circumferential direction, Fig. 8

ω_k angle of opening of the shell structure, Fig. 8

LIST OF REFERENCES

(1) Aas - Jakobsen, "Winddruck auf Bogenbrücken", Beton & Eisen 39
   (1940), p. 316.

(2) B. Thürlimann, R. Bereuter, B. Johnston; "Stress Distribution
   and Effective Width Adjacent to Stiffeners in
   Cylindrical Shells", Progress Report 213-A,
   October 1949.

(3) B. Thürlimann, B. Johnston; "Stress Distribution and Effective
   Width Adjacent to Stiffeners in Cylindrical Shells",
   Progress Report 213-B, April 1950.

(4) W. Flügge; "Statik und Dynamik der Schalen", Springer Verlag,
   Berlin 1934.